Automatica 95 (2018) 122–136

Contents lists available at ScienceDirect

Automatica

journal homepage: www.elsevier.com/locate/automatica

Exponential regulation of the anti-collocatedly disturbed cage in a wave PDE-modeled ascending cable elevator☆

Ji Wang [a,b,c], Shu-Xia Tang [b,*], Yangjun Pi [a,c,*], Miroslav Krstic [b]

[a] State Key Laboratory of Mechanical Transmission, Chongqing University, Chongqing 400044, China
[b] Department of Mechanical and Aerospace Engineering, University of California, San Diego, La Jolla, CA 92093-0411, USA
[c] College of Automotive Engineering, Chongqing University, Chongqing 400044, China

ARTICLE INFO

Article history:
Received 22 February 2017
Received in revised form 22 December 2017
Accepted 16 April 2018
Available online 2 June 2018

Keywords:
Wave equation
Anti-collocated disturbance
Exponential disturbance attenuation
Backstepping
Active disturbance rejection control

ABSTRACT

In cable elevators, large axial vibrations appear when a cage subject to disturbance is lifted up via a compliant cable. The axial vibration dynamics can be described by a wave partial differential equation (PDE) on a time-varying spatial interval with an unknown boundary disturbance. In this paper, we design an output feedback controller actuating at the boundary anti-collocated with the disturbance to regulate the state on the uncontrolled boundary of the wave PDE based on the backstepping idea and the active disturbance rejection control (ADRC) approach. The control law uses the state and disturbance information recovered from the state observer and the disturbance estimator, respectively, which are constructed via limited boundary measurements. The exponential convergence of the state on the uncontrolled boundary and uniform boundedness of all states in the closed-loop system are proved by Lyapunov analysis. Effective vibration suppression in the cable elevator with the designed controller is verified via numerical simulation.

1. Introduction

1.1. Background

Cable elevators are widely used for transportation of heavy objects to a large height or depth in many industrial environments. For instance, a mining cable elevator is used to transport the cargos and miners between the ground and the working platform which is as deep as 2 km by a cage at the bottom of the cable (Kaczmarczyk & Ostachowicz, 2003, Wang, Pi et al., 2017). The external disturbances exerted on the cage, such as airflow, and the compliance property of cables would cause large vibrations, which would lead to the fatigue failure and degrade the performance of system (He & Ge, 2016). The vibrations are particularly obvious in the ascending process because the vibratory energy increases when the cable length is being shortened (Zhu & Ni, 2000). Therefore, in the ascending process of mining cable elevators, a controller acting at the head sheave to attenuate the disturbance and suppress the vibrations at the moving cage through a time-varying length cable is required. Mathematically, this means attenuation of an anti-collocated disturbance and regulation of the uncontrolled boundary state in a wave PDE on a time-varying interval.

1.2. PDE control systems with moving boundary

The stabilization problem of a cascaded system of a transport PDE and a nonlinear ordinary differential equation (ODE) where the moving boundary of the transport PDE depends on the boundary values of the PDE state itself was addressed in Bekiaris-Liberis and Krstic (2018). Control problem of the bizone model of the extruder consisting of the transport PDE and the ODE with a moving interface was solved in Diagne, Bekiaris-Liberis, and Krstic (2017). Output feedback control of the one-phase Stefan problem mathematically formulated as a 1-D diffusion PDE on a time-varying spatial interval described by an ODE was proposed in Koga, Diagne, and Krstic (2016). Stabilization of a cascade system of a nonlinear ODE and a wave PDE with a moving uncontrolled boundary was developed in Cai and Krstic (2016) by using the predictor-based feedback control. However, these research did not consider external disturbances which appear frequently in the industrial environments.

☆ This work is supported by National Basic Research Program of China [2014CB049404], National Natural Science Foundation of China (61773112), 2015 Chongqing University Postgraduates Innovation Project [CYD15023] and China Scholarship Council (CSC). The material in this paper was not presented at any conference. This paper was recommended for publication in revised form by Associate Editor Yoshihiko Miyasato under the direction of Editor Richard Middleton.

* Corresponding authors.
E-mail addresses: wangji@cqu.edu.cn (J. Wang), shuxia_tang@berkeley.edu (S.-X. Tang), cqpp@cqu.edu.cn (Y. Pi), krstic@ucsd.edu (M. Krstic).

https://doi.org/10.1016/j.automatica.2018.05.022
0005-1098/

1.3. PDE control systems with disturbances

Most current research about attenuation of disturbances in PDE systems focuses on disturbances collocated with control. Sliding mode control (SMC) was designed for heat, Euler–Bernoulli beam, and Schrödinger equations with boundary input disturbances in Guo and Jin (2013a), Guo and Liu (2014) and Wang, Liu, Ren, and Chen (2015). Adaptive control was used in output feedback asymptotic stabilization of 1-D wave equations that were subject to harmonic disturbances at the controlled end and at the measured output in Guo and Guo (2013a, 2013b, 2013c) respectively. Internal model principle (Francis & Wonham, 1976) on the basis of the estimation/cancellation strategy was utilized in the beam (Rebarber & Weiss, 2003). ADRC proposed by Han (2009) was developed in the state feedback or output feedback design of wave PDEs with matched disturbances in Feng and Guo (2017), Guo and Jin (2013b), Guo and Jin (2015), Guo and Zhou (2015), Tang, Guo, and Krstic (2014) and Zhou, Guo, and Wu (2016).

Compared with the above literature which focuses on the attenuation of collocated disturbances, the problem of anti-collocated disturbance attenuation would be more difficult. Actually, systems with anti-collocated disturbances are widespread in practical engineering systems. For example, the airflow disturbance at the cage is not collocated with the control input at the top floating sheave in a cable elevator. Some results on the attenuation of anti-collocated disturbances have been achieved in ODE systems. A generalized extended state observer (ESO) based control approach was proposed for ODE systems with mismatched uncertainties and non-integral chain form in Li, Yang, Chen, and Chen (2012). By using ADRC, desired performance was achieved for a class of multi-input multi-output (MIMO) lower-triangular nonlinear systems with mismatched uncertainties via state feedback in Xue and Huang (2014). ADRC was also applied in output tracking for a class of nonlinear ODE systems with vast matched and mismatched uncertainties in Guo and Wu (2017). Less literature exists on the problem of anti-collocated disturbance attenuation in PDE systems. A state feedback controller that practically stabilizes the Schrödinger equation-ODE cascade system in the presence of an unmatched disturbance which is assumed as small and measurable was presented in Kang and Fridman (2016). For the output feedback design problem which is more complicated, output reference tracking of a wave equation with an anti-collocated harmonic disturbance at a stable damping boundary via the output feedback controller was presented in Guo and Guo (2016). The output regulation problem for a wave equation with a harmonic anti-collocated disturbance at a free boundary was dealt with in Guo, Shao, and Krstic (2017). However, the authors of Guo et al. (2017) only focus on the attenuation of a harmonic disturbance with known frequencies in a fixed interval wave equation and only achieve the asymptotic convergence of the output state of the wave equation. The problem we deal with is more complex: attenuation of an anti-collocated general harmonic disturbance with unknown amplitudes and frequencies in a wave PDE on a time-varying interval, and ensuring the exponential convergence of this uncontrolled boundary state.

1.4. Main contributions

(1) We achieve attenuation of an anti-collocated disturbance in a wave equation on a time-varying interval, which is more challenging than the problem solved in Feng and Guo (2017) about attenuation of a collocated disturbance in a fixed-interval wave equation.
(2) We attenuate a general harmonic disturbance with unknown amplitudes and frequencies via designing a disturbance estimator convergent to the actual disturbance, while the only available result for anti-collocated disturbance attenuation in wave PDEs is (Guo et al., 2017) which deals with a harmonic disturbance with known frequencies.
(3) Moreover, we obtain the exponential convergence result instead of the asymptotic convergence result in Guo et al. (2017).
(4) This is the first result on output feedback exponential regulation for a payload which is driven through a varying-length cable and is subject to a general harmonic disturbance anti-collocated with the control.

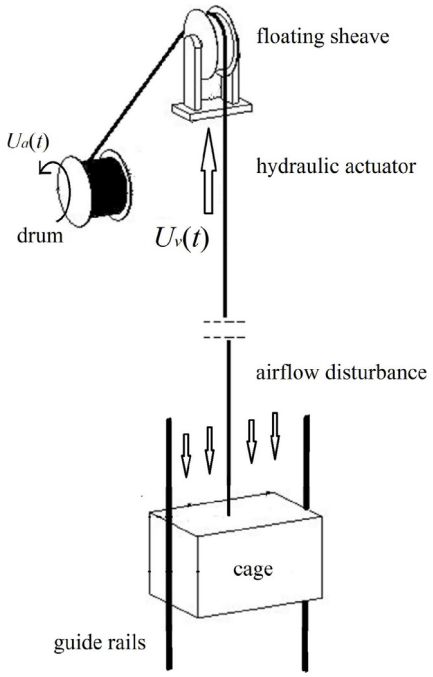

Fig. 1. The mining cable elevator.

1.5. Organization

The rest of the paper is organized as follows. The vibration dynamics of a cable elevator with an airflow disturbance at the moving cage is presented in Section 2. A disturbance estimator and a state observer for the wave PDE with the anti-collocated disturbance are designed in Section 3 and Section 4 respectively. In Section 5, we design the output feedback controller via the backstepping method (Krstic & Smyshlyaev, 2008), and prove the exponential convergence of the uncontrolled boundary state and uniform boundedness of all states in the closed-loop system. The simulation results are provided in Section 6. The conclusions and future work are presented in Section 7.

2. Problem formulation

The schematic of a mining cable elevator with an axial disturbance at the cage is depicted in Fig. 1. The drum drives the cable through the floating sheave to lift a cage which is subject to the disturbance. $U_v(t)$, where the subscript v denotes vibration, driven by the hydraulic actuator at the floating sheave is a control force to attenuate the disturbance and suppress vibrations. $U_a(t)$ at the drum is a separate control force to regulate motion dynamics.

The actual axial displacement $z^*(x, t)$ of each point in the cable can be considered as the sum of the motion $l(t)$ in the equal

Table 1
Physical parameters of the mining elevator.

Parameters (units)	Values
The time-varying length of the cable (m)	$l(t)$
Initial length (m)	L
Cable effective steel area (m^2)	A_a
Cable effective Young's modulus (N/m^2)	E
Cable linear density (kg/m)	ρ
Total hoisted mass (kg)	m
Maximum hoisting velocity (m/s)	$\bar{v}$

rigid-body model and the additional axial vibrations $u(x,t)$ of the compliant one, i.e., $z^*(x,t) = l(t) + u(x,t)$. $x \in [0, l(t)]$ denotes position coordinates along the cable in a moving coordinate system associated with the motion $l(t)$ where the origin is located at the cage at the initial moment. t represents time. Using Hamilton's principle (Mciver, 1973), a simplified dynamic model of axial vibration $u(x,t)$ can be built Wang, Koga, Pi and Krstic (2018) as follows,

$$u_{tt}(x,t) = q u_{xx}(x,t),\ \forall (x,t) \in (0,l(t)) \times (0,\infty),$$
$$\forall x \in (0,l(t)), \forall t \in (0,\infty), \tag{1}$$
$$u_x(0,t) = -\frac{m}{r}u_{tt}(0,t) - \frac{1}{r}d(t), \tag{2}$$
$$u_x(l(t),t) = U(t), \tag{3}$$

where the physical parameters are shown in Table 1 and $r = E \cdot A_a$, $q = E \cdot A_a/\rho$. $u(x,t)$ denotes the axial vibration displacements distributed in the cable. (2) describes the cage dynamics. (3) comes from $r u_x(l(t),t) = U_v(t)$ with the definition of $U_v(t) = rU(t)$, where $U(t)$ is the controller to be designed in this paper. $U_v(t)$ can be obtained via multiplying the designed $U(t)$ here by the constant gain r. Please refer to Wang, Koga, Pi and Krstic (2018) for the detailed modeling processes. The disturbance force $d(t)$ caused by airflow at the cage $x = 0$ is anti-collocated with the control input $U(t)$.

Remark 1. We ignore the effect of the vibration dynamics on the motion dynamics because the vibration displacement $u(x,t)$ is much smaller than the hoisting motion $l(t)$ from 2000 m under ground to the surface platform. Because the motion dynamics-$l(t)$ is regulated by the separate controller $U_a(t)$, we can consider that $l(t)$ from motion dynamics which is an independent ODE driven by $U_a(t)$ is the known hosting trajectory, and focus on the control design $U(t)$ of the PDE vibration dynamics (1)–(3), where $l(t)$ acts as a known time-varying function.

Remark 2. We only consider the airflow disturbance acting on the cage and ignore the ones acting at the cable. In fact, the axial vibration displacement is parallel to the direction of the airflow disturbance and the cross section of the cable is much smaller than that of the cage. Therefore, the airflow disturbance affects the cage more obviously.

Available measurements here are $\dot{u}(l(t),t)$, $u_{tt}(0,t)$ and $u(0,t)$. $\dot{u}(l(t),t)$ is at the controlled boundary, which can be directly obtained from the velocity feedback signals of the servo actuator acting at the floating sheave. The vibration acceleration $u_{tt}(0,t)$ is measured directly by an accelerometer placed at the cage, and then we obtain the vibration displacement $u(0,t)$ by integrating twice the measured acceleration with known initial conditions $u_t(0,0)$, $u(0,0)$. The control objective in this paper is to ensure the exponential convergence of $u(0,t)$ and the uniform boundedness of all states in the closed-loop system with the controller realized by the hydraulic actuator.

Assumption 1. $l(t) \in C^2(0,\infty)$. The ascending process of the cable elevator is concerned, which implies $l(t)$ is decreasing. Moreover, $l(t)$ is bounded: $0 < \underline{l} \le l(t) \le L, \forall t \ge 0$, where L denotes the initial length of the cable and $\underline{l} := \lim_{t\to\infty} l(t)$.

Assumption 2. The hoisting velocity $\dot{l}(t)$ is bounded:

$$-\bar{v} \le \dot{l}(t) \le 0,$$

where $\bar{v}$ which is the maximum hoisting velocity satisfies $\bar{v} \le \sqrt{q}$.

Note: in the mining cable elevator, the value of $\sqrt{q} = r/\rho = 7.5 \times 10^3$ is much larger than the value of the maximum hoisting velocity $\bar{v} = 18$ m/s, thus $\bar{v} < \sqrt{q}$. According to the conclusion in Gugat (2007a, 2007b), the fact that the derivative of the moving boundary $\dot{l}(t)$ is smaller than the wave speed $\sqrt{q}$ allows to prove a well-posedness result for the initial boundary value problem (1)–(3).

Assumption 3. The disturbance $d(t)$ is of the general harmonic form as

$$d(t) = \sum_{j=1}^{N} [\bar{a}_j \cos(\alpha_j t) + \bar{b}_j \sin(\alpha_j t)], \tag{4}$$

where N is an arbitrary positive integer. The amplitudes $\bar{a}_j$, $\bar{b}_j$, and frequencies α_j are arbitrary and unknown constants.

Then the disturbance $d(t)$ is bounded by constant lower and upper bounds as $|d(t)| \le \overline{D}$, where $\overline{D}$ is an arbitrary and unknown constant.

Because the periodic disturbance may cause resonance and thus result to serious vibrations in the flexible/compliant structure, it needs to be attenuated. The general harmonic form (4) covers almost all periodic signals. Therefore, Assumption 3 is reasonable.

3. Disturbance estimator design

The disturbance estimation is a key step in active disturbance rejection control. For the disturbed wave PDE (1)–(3) without the second order term in (2), Wang, Tang, Pi, and Krstic (2017) poses an estimator for the disturbance, based on which we build a disturbance estimator in this section for (1)–(3) by using the available measurements $\dot{u}(l(t),t)$ $u(0,t)$ and $u_{tt}(0,t)$.

Considering (2), the disturbance $d(t)$ can be tracked by estimating the boundary state $u_x(0,t)$ due to $u_{tt}(0,t)$ being measurable. Thus we would like to build the disturbance estimator by copying the form of the plant and achieving an error system, derivative of which is still exponentially stable (because $d(t)$ is connected with $u_x(0,t)$). We achieve the error system through building the estimator including two subsystems $\bar{u}(x,t)$ and $\bar{d}(x,t)$.

The $\bar{u}$-subsystem is built as

$$\bar{u}_{tt}(x,t) = q\bar{u}_{xx}(x,t), \tag{5}$$
$$\bar{u}_x(0,t) = -\frac{m}{r}u_{tt}(0,t), \tag{6}$$
$$\bar{u}_x(l(t),t) = (1 - a_1\dot{l}(t))U(t) + a_1\dot{u}(l(t),t) - a_1\bar{u}_t(l(t),t), \tag{7}$$

where the constant a_1 is to be determined later.

Note that substituting the relation $\dot{u}(l(t),t) = u_t(l(t),t) + \dot{l}(t)u_x(l(t),t)$ into (7) and recalling (3), (7) is equal to

$$\bar{u}_x(l(t),t) = U(t) + a_1(u_t(l(t),t) - \bar{u}_t(l(t),t)). \tag{8}$$

The original plant (1)–(3) subtracts the $\bar{u}$-subsystem yielding the following intermediate error system $\acute{u}(x,t) = u(x,t) - \bar{u}(x,t)$

$$\acute{u}_{tt}(x,t) = q\acute{u}_{xx}(x,t), \tag{9}$$
$$\acute{u}_x(0,t) = -\frac{1}{r}d(t), \tag{10}$$

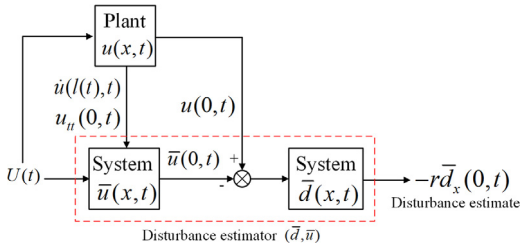

Fig. 2. Block diagram of the disturbance estimator.

$$\acute{u}_x(l(t),t) = -a_1\acute{u}_t(l(t),t), \tag{11}$$

where the disturbance $d(t)$ shows up in (10) and the other boundary is constructed as a damping type.

The following lemma shows the uniform boundedness of the $\acute{u}(x,t)$ system, which is crucial to ensure all internal subsystems of the disturbance estimator are uniformly bounded. The proof is shown in the Appendix.

Lemma 1. *For any initial values* $(\acute{u}(\cdot,0), \acute{u}_t(\cdot,0)) \in H^1(0,L)\times L^2(0,L)$, *defining the system norm*

$$(\|\acute{u}_t(\cdot,t)\|^2 + \|\acute{u}_x(\cdot,t)\|^2)^{1/2}, \tag{12}$$

where $\|\cdot\|$ *denotes* L^2*-norm, then the system (9)–(11) is uniformly bounded in the sense of*

$$\sup_{t\geq 0}(\|\acute{u}_t(\cdot,t)\|^2 + \|\acute{u}_x(\cdot,t)\|^2) \leq \frac{V_{\acute{u}}(0)}{\theta_{\acute{u}1}},$$

where $V_{\acute{u}}(0)$ *and* $\theta_{\acute{u}1}$ *are positive constants.*

Considering (10), we build the other $\bar{d}$-subsystem to exponentially recover the intermediate error system $\acute{u}$ and its derivative $\acute{u}_t$. The $\bar{d}$-subsystem is designed based on a copy of the $\acute{u}$-system (9)–(11) as:

$$\bar{d}_{tt}(x,t) = q\bar{d}_{xx}(x,t), \tag{13}$$

$$\bar{d}(0,t) = u(0,t) - \bar{u}(0,t), \tag{14}$$

$$\bar{d}_x(l(t),t) = -a_1\bar{d}_t(l(t),t), \tag{15}$$

where (14) ensures $\bar{d}(0,t) = \acute{u}(0,t)$ which is an important condition to obtain that the final error system $u(x,t) - \bar{u}(x,t) - \bar{d}(x,t)$ and its derivative are exponentially stable.

Based on the $\bar{d}$-subsystem (13)–(15), we define the disturbance estimation $\hat{d}(t)$ as

$$\hat{d}(t) = -r\bar{d}_x(0,t). \tag{16}$$

The process of estimating the disturbance is shown in Fig. 2.

Note that the cascaded PDE systems Eqs. (5)–(7) and (13)–(15) are completely known, since it is determined by the input and outputs of the original system (1)–(3), i.e., $U(t)$, $\dot{u}(l(t),t)$, $u(0,t)$ and $u_{tt}(0,t)$.

The following theorem tells us the disturbance estimation defined in (16) can track the actual disturbance $d(t)$ exponentially.

Theorem 1. *The error* $\tilde{d}(t)$ *between the disturbance estimation* $\hat{d}(t)$ *(16) defined by (5)–(7), (13)–(15), and the actual disturbance* $d(t)$ *is exponentially convergent in the sense of the following equation:*

$$\left|\tilde{d}(t)\right| = \left|d(t) - \hat{d}(t)\right| \leq \mu_{\tilde{d}}e^{-\sigma_{\tilde{d}}t}, \forall t \geq 0,$$

where $\sigma_{\tilde{d}} > 0$ *depends on* a_1 *and* $\mu_{\tilde{d}}$ *is a positive constant which depends on the initial values only.*

Then we present two lemmas which are useful to complete the proof of Theorem 1. The first lemma tells us that $\bar{d}(x,t)$ is exponentially convergent to $\acute{u}(x,t)$. The proof is shown in the Appendix.

Lemma 2. *For any initial values* $(\tilde{v}(\cdot,0), \tilde{v}_t(\cdot,0))$ *which belong to* $H^1(0,L)\times L^2(0,L)$, *the error state* $\tilde{v}(x,t) = \acute{u}(x,t) - \bar{d}(x,t)$ *is exponentially stable in the sense of the norm*

$$\left(\|\tilde{v}_t(\cdot,t)\|^2 + \|\tilde{v}_x(\cdot,t)\|^2\right)^{1/2}, \tag{17}$$

where the decay rate depends on a_1.

Based on Lemma 2, the second lemma states that $\bar{d}_t(x,t)$ is exponentially convergent to $\acute{u}_t(x,t) = u_t(x,t) - \bar{u}_t(x,t)$, from which $\bar{d}_x(0,t)$ governed by (13)–(15) can be proved exponentially convergent to $\acute{u}_x(0,t)$ by using Cauchy–Schwarz inequality. The proof is shown in the Appendix.

Lemma 3. *If any initial values* $(e(\cdot,0), e_t(\cdot,0))$ *which belong to* $H^1(0,L)\times L^2(0,L)$, *for some* a_1, *the system* $e(x,t) = \tilde{v}_t(x,t)$ *is exponentially stable in the sense of the norm*

$$\left(\|e_t(\cdot,t)\|^2 + \|e_x(\cdot,t)\|^2\right)^{1/2}. \tag{18}$$

Then we obtain $|\tilde{v}_x(0,t)| \leq \mu_{\tilde{v}}e^{-\sigma_{\tilde{d}}t}, \forall t \geq 0$, *where* $\sigma_{\tilde{d}} > 0$ *and* $\mu_{\tilde{v}}$ *is a positive constant which only depends on the initial values.*

With Lemma 3, we can then prove Theorem 1.

Proof of Theorem 1. According to (16) and (10), the estimation error of the proposed disturbance estimator can be obtained as

$$\tilde{d}(t) = d(t) - \hat{d}(t) = -r\acute{u}_x(0,t) + r\bar{d}_x(0,t) = -r\tilde{v}_x(0,t). \tag{19}$$

According to Lemma 3, we can conclude Theorem 1. Theorem 1 can be regarded as an independent contribution about exponentially tracking disturbances in time-varying interval wave PDEs.

In addition to the exponential convergence result of $\tilde{d}(t)$ proved in Theorem 1, moreover, we obtain the exponential convergence estimates of $\dot{d}(t)$, $\ddot{d}(t)$ in the following lemma by using the following assumption. The proof is shown in the Appendix.

Assumption 4. The hoisting acceleration $\ddot{l}(t) = 0$.

Assumption 4 is reasonable because the hoisting trajectory $l(t)$ can be considered as the uniform motion.

Lemma 4. *For any initial values* $(\tilde{v}_t(\cdot,0), \tilde{v}_{xx}(\cdot,0)) \in H^3(0,L)\times H^2(0,L)$, *the derivatives* $\dot{\tilde{d}}(t)$, $\ddot{\tilde{d}}(t)$ *of the estimation error* $\tilde{d}(t)$ *are exponentially convergent to zero.*

Furthermore, we can estimate each sinuous component in the harmonic disturbance (4) by using the disturbance estimation (16) in the following steps.

Define

$$Z(t)_{2N\times 1} = \left[\bar{a}_1\cos(\alpha_1 t), \bar{b}_1\sin(\alpha_1 t), \ldots, \bar{a}_N\cos(\alpha_N t), \bar{b}_N\sin(\alpha_N t)\right]^T, \tag{20}$$

the disturbance (4) can be written as

$$\ddot{Z}(t) = -A_z Z(t),\ d(t) = C_z Z(t), \tag{21}$$

where

$$A_z = \mathrm{diag}\left[\begin{pmatrix}\alpha_1^2 & 0\\ 0 & \alpha_1^2\end{pmatrix}, \ldots, \begin{pmatrix}\alpha_N^2 & 0\\ 0 & \alpha_N^2\end{pmatrix}\right],$$

$$C_z = [1, \ldots, 1]_{1\times 2N}.$$

According to the exponentially convergent disturbance estimation $\hat{d}(t) = -r\bar{d}_x(0,t)$ in Theorem 1, the matrix A_z consisting of the disturbance frequency components α_j is known, because the frequency components of the disturbance estimation $\hat{d}(t)$ are considered to be equal to those of the actual periodic disturbance $d(t)$ after eliminating the high-frequency noise with an appropriate cut-off frequency, which can be seen in Fig. 5. In practice, we can use the real-time spectrum analyzer to obtain the frequency components $\alpha_j, j = 1, 2, \ldots, N$ by analyzing the signal $-r\bar{d}_x(0,t)$.

Define $Y(t) = [\dot{Z}(t)^T, Z(t)^T]^T$, (21) can be written as

$$\dot{Y}(t) = \hat{A}_z Y(t),\ d(t) = \hat{C}_z Y(t), \tag{22}$$

with

$$\hat{A}_z = \begin{pmatrix} 0 & -A_z \\ I & 0 \end{pmatrix}_{4N\times 4N},\ \hat{C}_z = [0, C_z]_{1\times 4N}, \tag{23}$$

where I is an identity matrix with the appropriate dimension and $(\hat{A}_z, \hat{C}_z)$ is observable.

Using the disturbance estimation $\hat{d}(t)$ defined in (16), we can design an observer to estimate the state $Y(t)$ including sinuous components of the harmonic disturbance. The observer is considered as

$$\dot{\hat{Y}}(t) = \hat{A}_z\hat{Y}(t) + L_z(\hat{d}(t) - \hat{y}(t)),\ \hat{y}(t) = \hat{C}_z\hat{Y}(t), \tag{24}$$

where L_z is designed to make $\hat{A}_z - L_z\hat{C}_z$ Hurwitz.

Subtracting (24) from (22), we obtain the error system $\tilde{Y}(t) = Y(t) - \hat{Y}(t)$:

$$\dot{\tilde{Y}}(t) = (\hat{A}_z - L_z\hat{C}_z)\tilde{Y}(t) + L_z\tilde{d}(t), \tag{25}$$

$$\tilde{y}(t) = \hat{C}_z\tilde{Y}(t). \tag{26}$$

The following lemma holds.

Lemma 5. *The error $\tilde{Y}(t)$-system (25)–(26) is exponentially stable.*

Proof. According to the exponential convergence of $\tilde{d}(t)$ proved in Theorem 1, recalling $\hat{A}_z - L_z\hat{C}_z$ is Hurwitz, it is straightforward to prove the exponential stability of the $\tilde{Y}(t)$-system (25)–(26).

Remark 3. According to Lemma 5, defining

$$\hat{Z}(t) = \hat{C}\hat{Y}(t), \tag{27}$$

with $\hat{C} = [0, \mathrm{diag}(C_z)]_{2N\times 4N}$, we can state that $\tilde{Z}(t) = Z(t) - \hat{Z}(t) = \hat{C}Y(t) - \hat{C}\hat{Y}(t) = \hat{C}\tilde{Y}(t)$ is exponentially convergent to zero, which yields,

$$\frac{d\left|\tilde{Z}(t)\right|^2}{dt} = -\sigma_{\tilde{Z}}\left|\tilde{Z}(t)\right|^2, \tag{28}$$

where $\sigma_Z > 0$ depends on the exponential decay rate of the system-$\tilde{Y}$, and $||$ denotes Euclidean norm.

4. State observer design

With the disturbance estimator in Section 3, we can then design a state observer to reconstruct the distributed states. Recall that the control objective in this paper is to ensure the exponential convergence of $u(0,t)$. In addition to the challenges from the anti-collocated disturbance, the second order boundary condition (2) which is also anti-collocated with the control input in the system (1)–(3) poses difficulties to the control problem as well. A new variable $X(t) = [u(0,t), u_t(0,t)]^T$ is introduced to rewrite the system (1)–(3) as a PDE–ODE coupled (Tang & Xie, 2011; Zhou & Tang, 2012) system:

$$\dot{X}(t) = AX(t) + Bu_x(0,t) + \frac{1}{r}Bd(t), \tag{29}$$

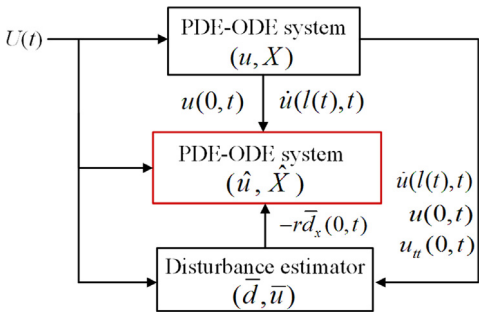

Fig. 3. Block diagram of the state observer.

$$u_{tt}(x,t) = qu_{xx}(x,t), \tag{30}$$

$$u(0,t) = CX(t), \tag{31}$$

$$u_x(l(t),t) = U(t), \tag{32}$$

with

$$A = \begin{bmatrix} 0 & 1 \\ 0 & 0 \end{bmatrix}, B = \frac{r}{m}\begin{bmatrix} 0 \\ -1 \end{bmatrix}, C = [1, 0], \tag{33}$$

where the boundary order is reduced and $CB = 0$. Note that the pair (A, B) is stabilizable and the pair (A, C) is observable.

In order to facilitate the design of observer-based output feedback control which depends on the construction of the observer, a copy of the plant (29)–(32) is used to build the observer by using the available measurements $u(0,t)$, $\dot{u}(l(t),t)$. Consider the observer as:

$$\dot{\hat{X}}(t) = A\hat{X}(t) + B\hat{u}_x(0,t) + \bar{L}(u(0,t) - C\hat{X}(t)) - B\bar{d}_x(0,t), \tag{34}$$

$$\hat{u}_{tt}(x,t) = q\hat{u}_{xx}(x,t), \tag{35}$$

$$\hat{u}(0,t) = u(0,t), \tag{36}$$

$$\hat{u}_x(l(t),t) = (1 - a_2\dot{l}(t))U(t) + a_2\dot{u}(l(t),t) - a_2\hat{u}_t(l(t),t), \tag{37}$$

where $\bar{d}_x(0,t)$ is governed by (13)–(15). a_2 is a positive damping gain and $\bar{L}$ is chosen to make $A - \bar{L}C$ Hurwitz.

Note that substituting the relation $\dot{u}(l(t),t) = u_t(l(t),t) + \dot{l}(t)u_x(l(t),t)$ into (37) and recalling (3), (37) is equal to

$$\hat{u}_x(l(t),t) = U(t) + a_2(u_t(l(t),t) - \hat{u}_t(l(t),t)). \tag{38}$$

Block diagram of the state observer is shown in Fig. 3.

Define the observer errors as

$$\tilde{u}(x,t) = u(x,t) - \hat{u}(x,t),\ \tilde{X}(t) = X(t) - \hat{X}(t). \tag{39}$$

Then the observer error system is

$$\dot{\tilde{X}}(t) = (A - \bar{L}C)\tilde{X}(t) + B\tilde{u}_x(0,t) + \frac{1}{r}B\tilde{d}(t), \tag{40}$$

$$\tilde{u}_{tt}(x,t) = q\tilde{u}_{xx}(x,t),\ \tilde{u}(0,t) = 0, \tag{41}$$

$$\tilde{u}_x(l(t),t) = -a_2\tilde{u}_t(l(t),t). \tag{42}$$

Define $\mathcal{H} = H^2(0,L) \times H^1(0,L)$. The following lemma holds, which tells the errors of the observer (34)–(37) are exponentially converge to zero. The proof is shown in the Appendix.

Lemma 6. *For any initial values $(\tilde{u}(\cdot,0), \tilde{u}_t(\cdot,0)) \in \mathcal{H}$, the $(\tilde{u}(x,t), \tilde{X}(t))$-system (40)–(42) is well-posed and exponentially stable in the sense of the norm*

$$\left(\left\|\tilde{u}_t(\cdot,t)\right\|^2 + \left\|\tilde{u}_x(\cdot,t)\right\|^2 + \left|\tilde{X}(t)\right|^2 + \left|\tilde{d}(t)\right|^2\right)^{\frac{1}{2}}, \tag{43}$$

where $|\cdot|$ denotes the Euclidean norm.

According to Lemma 6, we can state that the observer (34)–(37) exponentially converges to the original system (1)–(3).

Theorem 2. *For any initial values* $(\hat{u}(\cdot,0),\hat{u}_t(\cdot,0)) \in \mathcal{H}$, $(u(x,0), u_t(x,0)) \in \mathcal{H}$, *the observer* (34)–(37) *exponentially converges to the original system* (1)–(3) *in the sense of the norm*

$$\Big(\|u_t(\cdot,t)-\hat{u}_t(\cdot,t)\|^2+\|u_x(\cdot,t)-\hat{u}_x(\cdot,t)\|^2 + |u(0,t)-\hat{x}_1(t)|^2+|u_t(0,t)-\hat{x}_2(t)|^2\Big)^{\frac{1}{2}}. \tag{44}$$

where $[\hat{x}_1(t),\hat{x}_2(t)]^T=\hat{X}(t)$.

Proof. Considering Lemma 6, we have

$$\begin{aligned}&\|u_t(\cdot,t)-\hat{u}_t(\cdot,t)\|^2+\|u_x(\cdot,t)-\hat{u}_x(\cdot,t)\|^2\\&+|u(0,t)-\hat{x}_1(t)|^2+|u_t(0,t)-\hat{x}_2(t)|^2\\&\le\|\tilde{u}_t(\cdot,t)\|^2+\|\tilde{u}_x(\cdot,t)\|^2+\left|\tilde{X}(t)\right|^2+\left|\tilde{d}(t)\right|^2\le\mu_0 e^{-\sigma_{\tilde{u}}t},\end{aligned}$$

where the decay rate $\sigma_{\tilde{u}}>0$ and the positive constant μ_0 depends on the initial values $\|u_t(\cdot,0)-\hat{u}_t(\cdot,0)\|^2$, $\|u_x(\cdot,0)-\hat{u}_x(\cdot,0)\|^2$, $|u(0,0)-\hat{x}_1(0)|^2$, $|u_t(0,0)-\hat{x}_2(0)|^2$, $|d(0)-\hat{d}(0)|^2$.

The proof is completed.

5. Output feedback control design

We have built the disturbance estimator in Section 3 and the state observer in Section 4 with the measurements $u(0,t)$, $u_{tt}(0,t)$ and $\dot{u}(l(t),t)$. In this section, we would like to design an output feedback control law $U(t)$ by using the state and disturbance information recovered from the state observer and the disturbance estimator. The objective is to attenuate the disturbance at the end $x=0$ and regulate exponentially $u(0,t)$ by using the control input $U(t)$ at the other end $x=l(t)$. Because of (36), the objective can be achieved by guaranteeing the exponential convergence of $\hat{u}(0,t)$ in the state observer via designing a control input at the other boundary $x=l(t)$.

In the process of the controller design, we would like to convert the system (34)–(37) to an exponentially stable target PDE–ODE system without the disturbance terms. This conversion is achieved in two stages. In Section 5.1, the anti-collocated disturbance terms are moved to the other boundary collocated with the controller and $\hat{u}(0,t)=\hat{z}(0,t)$ is ensured via the first invertible transformation. In Section 5.2, the collocated disturbance terms are canceled and the exponentially stable target PDE–ODE coupled system is achieved via the second backstepping transformation.

5.1. Conversion from the system (34)–(37) to an intermediate system

We would like to transform the system (34)–(37) into the following intermediate system:

$$\begin{aligned}\dot{\hat{X}}(t)&=A\hat{X}(t)+B\hat{z}_x(0,t)+\bar{L}(u(0,t)-C\hat{X}(t))\\&\quad-\frac{1}{r}B\tilde{d}(t)+\frac{1}{r}BC_z\tilde{Z}(t),\end{aligned}\tag{45}$$

$$\hat{z}_{tt}(x,t)=q\hat{z}_{xx}(x,t)+\eta(x,t),\tag{46}$$

$$\hat{z}(0,t)=\hat{u}(0,t),\tag{47}$$

$$\hat{z}_x(l(t),t)=U(t)+a_2\tilde{u}_t(l(t),t)+\vartheta'(l(t))\hat{Z}(t),\tag{48}$$

where $\eta(x,t)$ and $\vartheta(x)$ will be defined later.

Note that the control and the anti-collocated disturbance are intentionally set to be collocated and $\hat{z}(0,t)$ is set to be equal to $\hat{u}(0,t)$ in the intermediate system (45)–(48). In the later derivation, the collocated disturbance can be then easily canceled through control input design. Moreover, we can get the exponential stability of the intermediate system (45)–(48) via designing a control law through the backstepping in the next stage, so that $\hat{u}(0,t)$ can be exponentially convergent to zero considering (47).

The transformation is defined as:

$$\hat{z}(x,t)=\hat{u}(x,t)+\vartheta(x)\hat{Z}(t).\tag{49}$$

(49) can be written as

$$\hat{z}(x,t)=\hat{u}(x,t)+\vartheta(x)Z(t)-\vartheta(x)\tilde{Z}(t).\tag{50}$$

Taking the second partial derivative of (50) with respect to x and t respectively, we get

$$\begin{aligned}&\hat{z}_{tt}(x,t)-q\hat{z}_{xx}(x,t)\\&=-\left(\vartheta(x)A_z+q\vartheta''(x)\right)Z(t)+q\vartheta''(x)\tilde{Z}(t)-\vartheta(x)\ddot{\tilde{Z}}(t).\end{aligned}\tag{51}$$

Define $\eta(x,t)$ in (46) as

$$\begin{aligned}\eta(x,t)&=q\vartheta''(x)\tilde{Z}(t)-\vartheta(x)\ddot{\tilde{Z}}(t)\\&=[q\vartheta''(x)\hat{C}-\vartheta(x)\hat{C}(\hat{A}_z-L_z\hat{C}_z)^2]\tilde{Y}(t)\\&\quad-\vartheta(x)\hat{C}(\hat{A}_z-L_z\hat{C}_z)L_z\tilde{d}(t)-\vartheta(x)\hat{C}L_z\dot{\tilde{d}}(t),\end{aligned}\tag{52}$$

where $\tilde{Z}(t)=\hat{C}\tilde{Y}(t)$ and (25) are used.

Then we obtain that $\vartheta(x)$ satisfies the ODE:

$$q\vartheta''(x)+\vartheta(x)A_z=0,\tag{53}$$

$$\vartheta'(0)=\frac{1}{r}C_z,\tag{54}$$

$$\vartheta(0)=0,\tag{55}$$

where (53) is obtained by comparing (51) with (46), and (54) is obtained via comparing (34) with the result from substituting (49) into (45) with (16), (21). For the boundary condition (47) to hold, the condition (55) is obtained.

Considering (53)–(55), the solution of $\vartheta(x)$ can be obtained as

$$\vartheta(x)=\frac{C_z}{r}\sqrt{\frac{q}{A_z}}\sin\left(\sqrt{\frac{A_z}{q}}x\right).\tag{56}$$

5.2. Conversion from the intermediate system (45) –(48) to a target system

In Section 5.1, we complete the conversion from the state observer (34)–(37) to the intermediate system (45)–(48) where the collocated disturbance can be easily canceled and $\hat{z}(0,t)=\hat{u}(0,t)$. Next, we would like to convert the intermediate system (45)–(48) to a target system via the PDE backstepping approach (Krstic, 2009).

The backstepping transformation is formulated as:

$$\begin{aligned}\hat{w}(x,t)&=\hat{z}(x,t)+\int_0^x\gamma(x,y)\hat{z}(y,t)dy\\&\quad+\int_0^x h(x,y)\hat{z}_t(y,t)dy+\beta(x)\hat{X}(t),\end{aligned}\tag{57}$$

where the kernel functions $\gamma(x,y)$, $h(x,y)$ and $\beta(x)$ in (57) are to be determined.

The target system is

$$\begin{aligned}\dot{\hat{X}}(t)&=(A+BK)\hat{X}(t)+B\hat{w}_x(0,t)-\frac{1}{r}B\tilde{d}(t)\\&\quad+(\bar{L}C-B\gamma(0,0)C)\tilde{X}(t)+\frac{1}{r}BC_z\tilde{Z}(t),\end{aligned}\tag{58}$$

$$\hat{w}_{tt}(x,t)=q\hat{w}_{xx}(x,t)-\bar{f}_1(x)\tilde{X}(t)+\bar{\eta}(x,t),\tag{59}$$

$$\hat{w}(0,t)=C\tilde{X}(t),\tag{60}$$

$$\hat{w}_x(l(t),t) = -a_3\hat{w}_t(l(t),t), \tag{61}$$

where a_3 in (61) is a positive damping gain and K in (58) is chosen to make $A+BK$ Hurwitz. $\bar{f}_1(x)$ in (59) is defined as

$$\bar{f}_1(x) = \beta(x)\bar{L}C(A-\bar{L}C) + \beta(x)A\bar{L}C + q\gamma_y(x,0)C + qh_y(x,0)C\bar{L}C + qh_y(x,0)CA.$$

$\bar{\eta}(x,t)$ in (59) is

$$\bar{\eta}(x,t) = \eta(x,t) + \int_0^x \gamma(x,y)\eta(y,t)dy + \int_0^x h(x,y)\eta_t(y,t)dy. \tag{62}$$

Applying Cauchy–Schwarz inequality into (62), we have

$$\begin{aligned}|\bar{\eta}(x,t)| &\le \max_{0\le x\le L}\{|C_2(x)|, |C_3(x)|, |C_4(x)|, |C_5(x)|\} \\ &\quad\times\left(\left|\tilde{Y}(t)\right| + \left|\tilde{d}(t)\right| + \left|\dot{\tilde{d}}(t)\right| + \left|\ddot{\tilde{d}}(t)\right|\right) \\ &= C_{max}\bar{\eta}_m(t),\end{aligned} \tag{63}$$

where (52) is used and $C_2(x)$, $C_3(x)$, $C_4(x)$, $C_5(x)$ are some bounded gains. C_{max} is a positive constant.

Recalling Theorem 1, Lemma 4 and Lemma 5, we have the signal $\bar{\eta}_m(t)$ is exponentially convergent to zero, which yields

$$\dot{\bar{\eta}}_m(t)^2 = -\sigma_{\bar{\eta}}\bar{\eta}_m(t)^2, \tag{64}$$

where $\sigma_{\bar{\eta}} > 0$. We thus get $\bar{\eta}(x,t)$ is exponentially convergent via (63).

The following lemma tells us the target system (58)–(61) is well-posed and exponentially stable. The proof is shown in the Appendix.

Lemma 7. *For any initial values $(\hat{w}(\cdot,0), \hat{w}_t(\cdot,0)) \in \mathcal{H}$, the target system (58)–(61) is well-posed and exponentially stable in the sense of the norm*

$$\left(\|\hat{w}_t(\cdot,t)\|^2 + \|\hat{w}_x(\cdot,t)\|^2 + \left|\hat{X}(t)\right|^2 + \left|\bar{\eta}_m(t)\right|^2 + \left|\tilde{d}(t)\right|^2 + \left|\tilde{Z}(t)\right|^2\right)^{\frac{1}{2}}. \tag{65}$$

By matching the system (45)–(48) with the system (58)–(61) through (57), we obtain the conditions for the kernels to be determined in the transformation (57) as:

$$\gamma_{xx}(x,y) = \gamma_{yy}(x,y), \quad \frac{d}{dx}\gamma(x,x) = 0, \tag{66}$$

$$\gamma(x,0) = \frac{1}{q}\beta(x)AB + h_y(x,0)CB, \tag{67}$$

$$h_{xx}(x,y) = h_{yy}(x,y), \tag{68}$$

$$h(x,0) = \frac{1}{q}\beta(x)B, \quad \frac{d}{dx}h(x,x) = 0, \tag{69}$$

$$\beta''(x) = \frac{1}{q}\beta(x)A^2 + \gamma_y(x,0)C + h_y(x,0)CA, \tag{70}$$

$$\beta'(0) = K - \gamma(0,0)C - h(0,0)CA, \ \beta(0) = -C, \tag{71}$$

which is a coupled system of an ODE and two PDEs. According to (66)–(71), the kernel functions $\gamma(x,y)$, $h(x,y)$ and $\beta(x)$ in (57) can be computed as

$$\gamma(x,y) = \frac{1}{q}\begin{bmatrix}-C & \Lambda - K\end{bmatrix}e^{D(x-y)}\begin{bmatrix}I\\0\end{bmatrix}AB, \tag{72}$$

$$h(x,y) = \frac{1}{q}\begin{bmatrix}-C & \Lambda - K\end{bmatrix}e^{D(x-y)}\begin{bmatrix}I\\0\end{bmatrix}B, \tag{73}$$

$$\beta(x) = \begin{bmatrix}-C & \Lambda - K\end{bmatrix}e^{Dx}\begin{bmatrix}I\\0\end{bmatrix}, \tag{74}$$

where I denotes the identity matrix of the appropriate dimension and D, Λ are defined as

$$D = \begin{bmatrix}0 & \frac{1}{q}A^2\\ I & -\frac{1}{q}(BCA+ABC)\end{bmatrix}, \quad \Lambda = \frac{1}{q}CABC.$$

Similarly, the inverse transformation of (57) can be obtained.

For the boundary condition (61) to hold, the controller $U(t)$ can be obtained as

$$\begin{aligned}U(t) = \frac{1}{c_1}\Bigg(&c_2\hat{z}_t(l(t),t) + f_3(l(t))\hat{z}(l(t),t) \\ &+ f_4(l(t))\hat{z}_x(0,t) + f_5(l(t))\hat{z}(0,t) + f_6(l(t))\hat{X}(t) \\ &+ \int_0^{l(t)} f_7(l(t),x)\hat{z}(x,t)dx + \int_0^{l(t)} f_8(l(t),x)\hat{z}_t(x,t)dx\Bigg) \\ &- a_2\tilde{u}_t(l(t),t) - \vartheta'(l(t))\hat{Z}(t),\end{aligned} \tag{75}$$

where

$$c_1 = 1 - a_3KB, \ \ c_2 = -a_3, \tag{76}$$

$$f_3(l(t)) = \gamma(l(t),l(t)) - qh_{xy}(l(t),l(t)), \tag{77}$$

$$f_4(l(t)) = a_3qh_x(l(t),0) - a_3\beta(l(t))B, \tag{78}$$

$$f_5(l(t)) = qa_3h_{xy}(l(t),0), \tag{79}$$

$$f_6(l(t)) = \beta_x(l(t)) + a_3\beta(l(t))A, \tag{80}$$

$$f_7(l(t),x) = \gamma_x(l(t),x) + qh_{xyy}(l(t),x), \tag{81}$$

$$f_8(l(t),x) = h_x(l(t),x) + a_3\gamma(l(t),x). \tag{82}$$

The following lemma tells us that the closed-loop system-$(\hat{z},\hat{X})$ is exponentially stable, which will be used in the proof of the exponential convergence of $u(0,t)$ in the original system because the $(\hat{z},\hat{X})$ system and the original system are connected at $x=0$.

Lemma 8. *For any initial values $(\hat{z}(\cdot,0), \hat{z}_t(\cdot,0)) \in \mathcal{H}$, the system-$(\hat{z},\hat{X})$ consisting of the plant (45)–(48) and the control law (75) is exponentially stable in the sense of the norm*

$$\left(\|\hat{z}_t(\cdot,t)\|^2 + \|\hat{z}_x(\cdot,t)\|^2 + \left|\hat{X}(t)\right|^2\right)^{1/2}.$$

Proof. Based on Lemma 7 and the invertibility and continuity of the transformation (57), the proof is straightforward.

5.3. Stability of closed-loop system

Controller (75) can be written by $\hat{u}$ and the available measurements as

$$\begin{aligned}U(t) = \frac{1}{(1+a_2|\dot{l}(t)|)}\Bigg[&\frac{1}{c_1}\Bigg(c_2\hat{u}_t(l(t),t) + f_3(l(t))\hat{u}(l(t),t) \\ &+ f_4(l(t))\hat{u}_x(0,t) + f_5(l(t))\hat{u}(0,t) \\ &+ f_6(l(t))\hat{X}(t) + \int_0^{l(t)} f_7(l(t),x)\hat{u}(x,t)dx \\ &+ \int_0^{l(t)} f_8(l(t),x)\hat{u}_t(x,t)dx\Bigg) - a_2\dot{u}(l(t),t) \\ &+ a_2\hat{u}_t(l(t),t) + r\mathcal{L}(l(t))\hat{C}L_z\bar{d}_x(0,t) \\ &- [\mathcal{P}(l(t)) + \mathcal{L}(l(t))(\hat{A}_z - L_z\hat{C}_z)\hat{C}]\hat{Z}(t)\Bigg],\end{aligned} \tag{83}$$

where

$$\mathcal{P}(l(t)) = \left[\frac{f_3(l(t))}{c_1}\vartheta(l(t)) + \frac{f_4(l(t))}{c_1}\right.$$

$$+\int_0^{l(t)}\frac{f_7(l(t),x)}{c_1}\vartheta(x)dx+\vartheta'(l(t))\Big], \tag{84}$$

$$\mathcal{L}(l(t))=\Big[\frac{c_2}{c_1}\vartheta(l(t))+\int_0^{l(t)}\frac{f_8(l(t),x)}{c_1}\vartheta(x)dx\Big]. \tag{85}$$

All signals required in the control law (83) are obtained from the measurable boundary quantities $\dot{u}(l(t),t)$, $u(0,t)$ and $u_{tt}(0,t)$. In detail, $\dot{u}(l(t),t), u(0,t)$ are used to construct the observer (34)–(37) to estimate the distributed states $u(x,t)$ and $X(t)$, i.e., to obtain $\hat{u}(x,t), \hat{X}(t)$. The measurements $\dot{u}(l(t),t)$, $u(0,t)$ and $u_{tt}(0,t)$ are also used to build the disturbance estimator (5)–(7) and (13)–(15) to obtain the disturbance estimation $\hat{d}(t)=-r\bar{d}_x(0,t)$ which is used to get $\hat{Z}(t)$ based on (24)–(27). In practice, the estimator and the observer can be calculated by using the finite discretization method, where different spatial steps are to be chosen by considering the tradeoff between the model accuracy and the computation speed in different cases and the time step depends on the sample period of the data acquisition.

Considering the controller (83), which uses the information from the disturbance estimator in Section 3 and the state observer in Section 4, the closed-loop system is built as

$$u_{tt}(x,t)=qu_{xx}(x,t), \tag{86}$$

$$u_x(0,t)=-\frac{m}{r}u_{tt}(0,t)-\frac{1}{r}d(t), \tag{87}$$

$$u_x(l(t),t)=U(t), \tag{88}$$

$$\dot{\hat{X}}(t)=A\hat{X}(t)+B\hat{u}_x(0,t)+\bar{L}(u(0,t)-C\hat{X}(t))-B\bar{d}_x(0,t), \tag{89}$$

$$\hat{u}_{tt}(x,t)=q\hat{u}_{xx}(x,t), \tag{90}$$

$$\hat{u}(0,t)=u(0,t), \tag{91}$$

$$\hat{u}_x(l(t),t)=(1-a_2\dot{l}(t))U(t)+a_2\dot{u}(l(t),t)-a_2\hat{u}_t(l(t),t), \tag{92}$$

$$\bar{d}_{tt}(x,t)=q\bar{d}_{xx}(x,t),\ \bar{d}(0,t)=u(0,t)-\bar{u}(0,t), \tag{93}$$

$$\bar{d}_x(l(t),t)=-a_1\bar{d}_t(l(t),t), \tag{94}$$

$$\bar{u}_{tt}(x,t)=q\bar{u}_{xx}(x,t),\ \bar{u}_x(0,t)=-\frac{m}{r}u_{tt}(0,t), \tag{95}$$

$$\bar{u}_x(l(t),t)=(1-a_1\dot{l}(t))U(t)+a_1\dot{u}(l(t),t)-a_1\bar{u}_t(l(t),t), \tag{96}$$

$$\dot{\hat{Y}}(t)=(\hat{A}_z-L_z\hat{C}_z)\hat{Y}(t)-L_zr\bar{d}_x(0,t), \tag{97}$$

$$\hat{Z}(t)=\hat{C}\hat{Y}(t), \tag{98}$$

where $U(t)$ is shown in (83)–(85). $\hat{X}(t), \hat{Z}(t)$ used in $U(t)$ are estimations of $X(t)=[u(0,t), u_t(0,t)]^T$ and $Z(t)$ (20) respectively.

We present next the main theorem of this paper.

Theorem 3. *The closed-loop system including the plant (86)–(88) with the unmatched disturbance $d(t)$, the disturbance estimator (93)–(96) and (97)–(98), the state observer (89)–(92) and the controller (83), has the following properties:*

(1) *The closed-loop system is well-posed.*

(2) *There exist positive constants μ_1 and σ such that the output state $u(0,t)$ of the closed-loop system is exponentially convergent to zero in the sense of*

$$|u(0,t)|\le\mu_1e^{-\sigma t},\forall t\ge 0.$$

(3) *All states in the closed-loop system are uniformly bounded in the sense of*

$$\sup_{t\ge0}\Big[\int_0^{l(t)}\Big(u_t^2(x,t)+u_x^2(x,t)+\hat{u}_t^2(x,t)+\hat{u}_x^2(x,t)+\bar{d}_t^2(x,t)+\bar{d}_x^2(x,t)+\bar{u}_t^2(x,t)+\bar{u}_x^2(x,t)\Big)dx+\left|\hat{X}(t)\right|^2+\left|\hat{Y}(t)\right|^2+\left|\hat{Z}(t)\right|^2\Big]<\infty. \tag{99}$$

(4) *The controller $U(t)$ (83) is bounded in the closed-loop system in the sense of*

$$\sup_{t\ge0}|U(t)|<\infty.$$

Proof.

Proof of (1): It is the direct consequence of the equivalence between the target system and the closed-loop system by recalling Lemmas 6 and 7.

Proof of (2): According to (47) and (91), we get the fact $u(0,t)=\hat{u}(0,t)=\hat{z}(0,t)$. This together with Lemma 8 from which we can state that $\hat{z}(0,t)$ is exponentially convergent with the decay rate σ, gives the property (2).

Proof of (3): According to Assumption 3 and Theorem 1, we have $\hat{d}=-r\bar{d}_x(0,t)$ is bounded. Then $\hat{Z}(t)$ obtained from (98) is bounded because $\hat{A}_z-L_z\hat{C}_z$ is Hurwitz in (97) which shows the boundedness of $\hat{Y}(t)$ considering the boundedness of $\hat{d}=-r\bar{d}_x(0,t)$. Together with Lemma 8 and the invertible transformation (49), we obtain that $(\hat{u}(x,t),\hat{X}(t))$ is uniformly bounded in the sense of (99). For the sake of brief, when we mention boundedness, it refers to the corresponding state norms in (99). Then from (39) with Lemma 6, we can state that $u(x,t)$ is uniformly bounded. Based on Lemma 1 which proves the uniform boundedness of the system $\acute{u}(x,t)$ and Lemma 2 which means the exponential stability of $\tilde{v}(x,t)$ system, we can get $\bar{d}(x,t)$ is uniformly bounded considering $\tilde{v}(x,t)=\acute{u}(x,t)-\bar{d}(x,t)$. Then we can obtain that $\bar{u}(x,t)$ is also uniformly bounded considering $\tilde{v}(x,t)=u(x,t)-\bar{u}(x,t)-\bar{d}(x,t)$. Therefore, all subsystems in the closed-loop system (86)–(98) are uniformly bounded as (99). Then we get the property (3).

Proof of (4): In the proof of the property (3), we have proved the boundedness of all states in the closed-loop system in the sense of (99). Now we prove the boundedness of the controller $U(t)$ (83). Considering (83) and the property (3) in Theorem 3, we know the boundedness analysis of four signals $\hat{u}_t(l(t),t)$, $\hat{u}_x(0,t)$, $u_x(l(t),t)$, $u_t(l(t),t)$ in (83) need to be conducted, which can be obtained by producing L_2 estimates of $u_{xx}(x,t)$, $u_{xt}(x,t)$, $\hat{u}_{xx}(x,t)$, $\hat{u}_{xt}(x,t)$, that is, $\|\tilde{u}_{xx}(\cdot,t)\|$, $\|\tilde{u}_{xt}(\cdot,t)\|$ and $\|\hat{u}_{xx}(\cdot,t)\|$, $\|\hat{u}_{xt}(\cdot,t)\|$.

Then we present two lemmas. The first one shows the bounded estimates in terms of $\|\hat{u}_{xx}(\cdot,t)\|^2+\|\hat{u}_{xt}(\cdot,t)\|^2$. The proof is shown in the Appendix. The second one gives the bounded estimates in terms of $\|\tilde{u}_{xx}(\cdot,t)\|^2+\|\tilde{u}_{xt}(\cdot,t)\|^2$.

Lemma 9. *If any initial values $(\hat{u}(\cdot,0),\hat{u}_t(\cdot,0))\in\mathcal{H}$, the system $\hat{u}(x,t)$ is bounded in the sense of $\left\|\hat{u}_{xx}(\cdot,t)\right\|^2+\left\|\hat{u}_{xt}(\cdot,t)\right\|^2$.*

Through the similar process in the proof of Lemma 9, it is straightforward to prove Lemma 10.

Lemma 10. *If any initial values $(\tilde{u}(\cdot,0),\tilde{u}_t(\cdot,0))\in\mathcal{H}$, the system $\tilde{u}(x,t)$ is bounded in the sense of $\left\|\tilde{u}_{xx}(\cdot,t)\right\|^2+\left\|\tilde{u}_{xt}(\cdot,t)\right\|^2$.*

Recalling the bounded estimate for the norm $\|\hat{u}_{xx}(\cdot,t)\|+\|\hat{u}_{xt}(\cdot,t)\|$ proved in Lemma 9 and using Sobolev inequality, we obtain that $\hat{u}_x(l(t),t)$, $\hat{u}_x(0,t)$ and $\hat{u}_t(l(t),t)$ are bounded.

Similarly, using Lemma 10, we obtain the boundedness of $\tilde{u}_x(l(t),t)$, $\tilde{u}_t(l(t),t)$.

According to the boundedness of $\hat{u}_x(0,t)$, $\hat{u}_x(l(t),t)$, $\hat{u}_t(l(t),t)$, $\tilde{u}_x(l(t),t)$, $\tilde{u}_t(l(t),t)$, we can obtain the boundedness of the four signals $\hat{u}_t(l(t),t)$, $\hat{u}_x(0,t)$, $u_x(l(t),t)$, $u_t(l(t),t)$ required for proving that $U(t)$ is bounded. Then we get the property (4).

Then we can conclude Theorem 3.

Table 2
Simulation parameters of the mining elevator.

Parameters	L	r	ρ	q	m
Values	2000	0.48×10^7	8.1	5.9×10^5	15 000

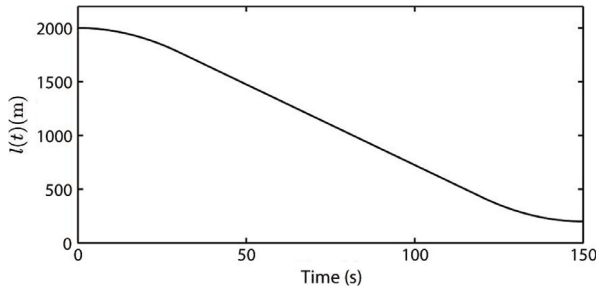

Fig. 4. The target hoisting trajectory $l(t)$.

6. Simulation

The system parameters of the mining cable elevator used in the simulation are shown in Table 2. Consider the cage subject to an airflow disturbance described as

$$d(t) = 150\sin(0.3t) + 100\sin(0.4t) + 200\cos(0.2t) + 140\cos(0.25t). \quad (100)$$

The simulation is performed based on a priori-known $l(t)$ in Fig. 4, which is considered as a monotonically decreasing curve from 2000 m to 200 m with the maximum velocity $\bar{v} = 15$ s during the total hoisting time 150 s.

The control force is multiplying the constant r and (83), with the gain functions (76)–(82) and (84)–(85) where kernels $\gamma(x, y)$, $h(x, y)$, $\beta(x)$, $\vartheta(x)$ are defined in (72)–(74) and (56) respectively. In the controller, the states $\hat{u}(x, t)$, $\hat{X}(t)$ are defined by the state observer (89)–(92). $\bar{d}_x(0, t)$ is defined by the disturbance estimator (93)–(96), $\hat{Z}(t)$ is defined by (97)–(98). Constant control parameters required in the controller are shown as following. $K = [k_1, k_2]$ are chosen as $[0.0012, 0.011]$. $\bar{L} = [l_1, l_2]$ are chosen as $[1.5, 1]$ and $L_z = [1, \cdots, 1]_{1\times 16}$. Other control parameters are $a_1 = 0.022$, $a_2 = 0.07$, $a_3 = 0.01$. The PDE on the time-varying domain $[0, l(t)]$ is converted to the one on the fixed domain $[0, 1]$ with time-varying coefficients via introducing $\check{\xi} = \frac{x}{l(t)}$, and then the simulation is conducted based on the finite difference method with the time step and the space step as 0.001 and 0.05 respectively.

By using the available boundary measurements $u(0, t)$, $u_{tt}(0, t)$ and $\dot{u}(l(t), t)$, the disturbance estimator (93)–(96) can be built with the initial conditions $\bar{d}(x, 0) = 0$ and $\bar{u}(x, 0) = 0$. Fig. 5 shows that the estimation from the disturbance estimator (93)–(96) can track the actual unknown disturbance (100) with fast tracking speed. Note that in practice the high frequency noise at the beginning of the estimation process can be eliminated with a low-pass filter by setting an appropriate cut-off frequency. The error between the estimated and actual values of the disturbance (100) is shown in Fig. 6. The estimated variables of the distributed states are obtained by the proposed observer (34)–(37) with available boundary measurements $u(0, t)$ and $\dot{u}(l(t), t)$. The initial errors of the observer are defined as 0.005 m. Because the locations of the actuator and the sensor are at the opposite boundaries, the estimation of the state at the midpoint $x = l(t)/2$ is most challenging due to its accessibility. Fig. 7 shows the observer error at the midpoint of the cable converges to zero quickly, which implies that the estimation from the state observer (34)–(37) can reconstruct their actual distributed states.

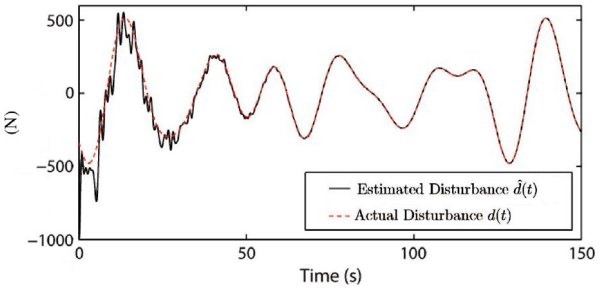

Fig. 5. The disturbance estimation $\hat{d}(t) = -r\bar{d}_x(0, t)$ and the actual disturbance $d(t)$ (100) (red dashed).

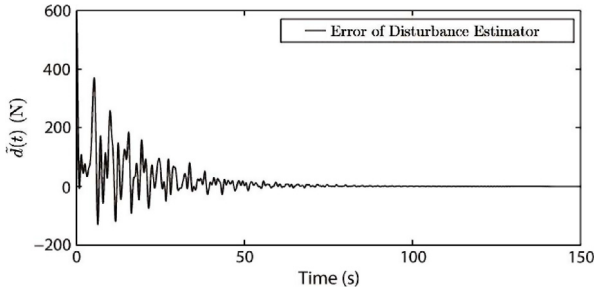

Fig. 6. The estimation error $\tilde{d}(t) = d(t) - \hat{d}(t)$ between the actual disturbance $d(t)$ (100) and the disturbance estimation $\hat{d}(t) = -r\bar{d}_x(0, t)$.

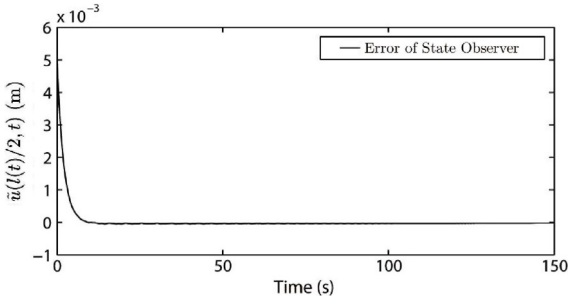

Fig. 7. The observer error $\tilde{u}(l(t)/2, t)$ at the midpoint of the cable.

The closed-loop responses under the proposed control law (83) and the proportional–derivative (PD) control law which is classical in industries are examined, to compare their performance on suppression of the axial vibrations at the cage. Consider the PD control law:

$$U_{\mathrm{pd}}(t) = k_{\mathrm{p}}u(l(t), t) + k_{\mathrm{d}}\dot{u}(l(t), t), \quad (101)$$

where k_{p}, k_{d} are gain parameters. The values of k_{p}, k_{d} are tuned to attain the efficient control performance. Here we choose $k_{\mathrm{p}} = 700$, $k_{\mathrm{d}} = 14000$. From Fig. 8, we can observe the oscillation appearing at the cage is becoming larger and larger because of the disturbance. Fig. 9 shows both the proposed output-feedback control law and the PD control can suppress the enlargement of the vibration displacement. Moreover, the proposed control law can regulate the vibration displacement $u(0, t)$ of the cage to zero with faster convergence and less overshoot despite of the disturbance at the cage. In addition, according to Fig. 10, we can see that the proposed control law also has better control performance for the interval state such as the midpoint $u(l(t)/2, t)$ of the cable. It means states in the interval can be uniformly bounded. Fig. 11 shows that the output feedback control input in the closed-loop system is uniformly bounded. Note that the control input is not zero at the

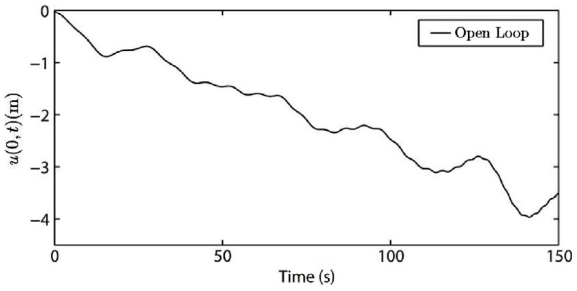

Fig. 8. The open loop response $u(0,t)$ of the plant (1)–(3) under the disturbance (100) at $x = 0$.

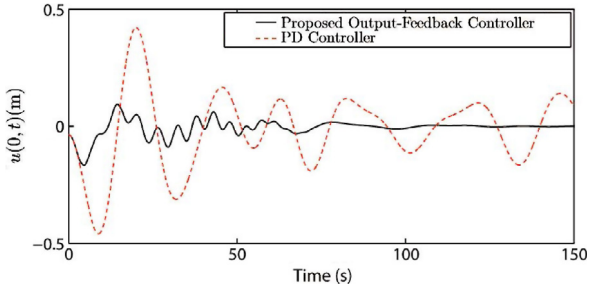

Fig. 9. The output responses $u(0,t)$ of the closed-loop system (86)–(98) under the disturbance (100) at $x = 0$ with the proposed output-feedback controller (83) (black line) and PD controller (101) (red dashed).

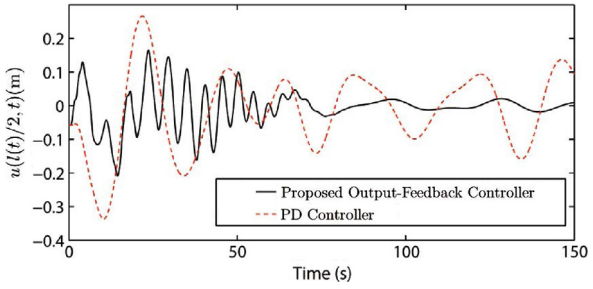

Fig. 10. The responses $u(l(t)/2,t)$ of the closed-loop system (86)–(98) under the disturbance (100) at $x = 0$ with the proposed output-feedback controller (83) (black line) and PD controller (101) (red dashed).

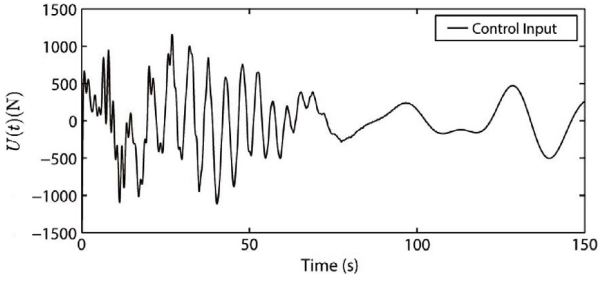

Fig. 11. The output feedback controller.

final moment $t = 150$ s because the disturbance in Fig. 5 is not zero at that time, so the attenuation behavior of the controller is continuing to ensure the convergence of the controlled states.

The model parameter error between the actual plant and the nominal plant often appears in practice. In order to test the robustness of the proposed controller to the model parameter error, we change some plant parameters with respect to their nominal

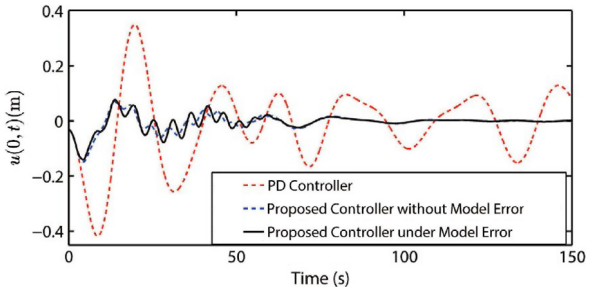

Fig. 12. The output responses $u(0,t)$ of the closed-loop system (86)–(98) under the disturbance (100) at $x = 0$ with the proposed output-feedback controller (83) under the model error (black line) and without the model error (blue dashed), and the PD controller (101) (red dashed).

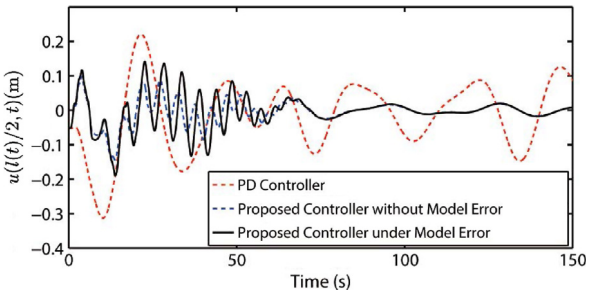

Fig. 13. The output responses $u(l(t)/2,t)$ of the closed-loop system (86)–(98) under the disturbance (100) at $x = 0$ with the proposed output-feedback controller (83) under the model error (black line) and without the model error (blue dashed), and the PD controller (101) (red dashed).

values in Table 2, such as $r = 0.56 \times 10^7$, $\rho = 8.5$, $q = r/\rho = 6.6 \times 10^5$ and $M = 15\,500$. These plant parameters are considered as actual plant parameters and those in Table 2 are nominal plant parameters, and the difference between them thus is the model error. For the actual plant, applying the proposed controller based on the nominal plant parameters (under the model error), the proposed controller based on the actual plant parameters (without the model error), and the PD controller with new control gains $k_p = 630$, $k_d = 15\,000$ which are tuned to attain efficient control performance, the comparing results are presented in Figs. 12 and 13 which show the vibration responses of the cage and the midpoint of the cable respectively. We can observe that although the vibration amplitudes under the proposed controller with the model error are slightly larger than the vibration amplitudes under the proposed controller without the model error before 65 s, both of them have the similar good results as time goes on and have the better performance than the standard PD controller.

7. Conclusions and future work

In this paper, we propose an output feedback control law for a wave PDE on a time-varying interval subject to a general harmonic disturbance with unknown amplitudes and frequencies, which is anti-collocated with the control input. The controller using the information from the state observer and the disturbance estimator actuates at one end $x = l(t)$ to attenuate the disturbance at the other end $x = 0$ and exponentially regulate the uncontrolled boundary state $u(0,t)$. Exponential convergence of $u(0,t)$ and uniform boundedness of all states in the closed-loop system are proved by the Lyapunov analysis. Physically the control system can be used in cable elevators to attenuate disturbances and suppress vibrations of a cage lifted up by a time-varying length cable.

In the future, the synchronism control of motion dynamics $l(t)$ and vibration dynamics $u(x,t)$ will be studied, where the constraint on the control input will be considered in the controller design (Isidori, Marconi, & Serrani, 2012). The distributed disturbances on the cable will also be considered in the estimator and controller design. Another interesting topic is how to obtain the optimal convergence rate by setting the feedback gains in the closed-loop system, which will also be studied.

Appendix

Proof of Lemma 1. Similar as in Krstic, Guo, Balogh, and Smyshlyaev (2008), we employ a Lyapunov function

$$V_{\acute{u}}(t) = \frac{1}{2}\left\|\acute{u}_t(\cdot,t)\right\|^2 + \frac{q}{2}\left\|\acute{u}_x(\cdot,t)\right\|^2 + \delta_{\acute{u}}\int_0^{l(t)}(1+x)\acute{u}_x(x,t)\acute{u}_t(x,t)dx, \tag{102}$$

where the parameter $\delta_{\acute{u}}$ is to be determined and needs to at least satisfy $0 < \delta_{\acute{u}} < 1/(1+L)\min\{1,q\}$ to guarantee the positive definiteness of $V_{\acute{u}}(t)$. Defining $\Omega_{\acute{u}}(t)$ as the square of the norm (12), we can get the inequality

$$\theta_{\acute{u}1}\Omega_{\acute{u}}(t) \le V_{\acute{u}}(t) \le \theta_{\acute{u}2}\Omega_{\acute{u}}(t), \tag{103}$$

where

$$\theta_{\acute{u}1} = \frac{1}{2}[\min\{1,q\} - \delta_{\acute{u}}(1+L)] > 0,$$
$$\theta_{\acute{u}2} = \frac{1}{2}[\max\{1,q\} + \delta_{\acute{u}}(1+L)] > 0.$$

Taking the derivative of $V_{\acute{u}}(t)$ along the system (9)–(11), applying Young's inequality and $0 < l(t) \le L$, choosing

$$0 < \delta_{\acute{u}} < \frac{1}{1+L}\min\left\{1, q, \frac{2a_1q}{1+qa_1{}^2}, \frac{1+qa_1^2}{2a_1}\right\}, \tag{104}$$

we obtain

$$\dot{V}_{\acute{u}} \le -\lambda_{\acute{u}}V_{\acute{u}} + \overline{M}, \tag{105}$$

where $\lambda_{\acute{u}} = \delta_{\acute{u}}/(2\theta_{\acute{u}2})$ and $\overline{M} = 1/r^2[1/(2r_1) - \delta_{\acute{u}}/2]\overline{D}^2$ with $0 < r_1 < \delta_{\acute{u}}/q^2$.

Multiplying both sides of (105) by $e^{\lambda_{\acute{u}}t}$, we obtain

$$\frac{d(V_{\acute{u}}e^{\lambda_{\acute{u}}t})}{dt} \le \overline{M}e^{\lambda_{\acute{u}}t}. \tag{106}$$

Integration of (106) yields

$$\Omega_{\acute{u}}(t) \le \frac{1}{\theta_{\acute{u}1}}V_{\acute{u}}(t) \le \frac{1}{\theta_{\acute{u}1}}(V_{\acute{u}}(0) - \frac{\overline{M}}{\lambda_{\acute{u}}})e^{-\lambda_{\acute{u}}t} + \frac{\overline{M}}{\theta_{\acute{u}1}\lambda_{\acute{u}}},$$

which implies $\Omega_{\acute{u}}(t)$ is uniformly bounded by $V_{\acute{u}}(0)/\theta_{\acute{u}1}$. Moreover, it is uniformly ultimately bounded with ultimate bound $\overline{M}/(\theta_{\acute{u}1}\lambda_{\acute{u}})$. The proof is completed.

Proof of Lemma 2. According to (9)–(11) and (13)–(15), the system $\tilde{v}$ is governed by

$$\tilde{v}_{tt}(x,t) = q\tilde{v}_{xx}(x,t), \tag{107}$$
$$\tilde{v}(0,t) = 0, \quad \tilde{v}_x(l(t),t) = -a_1\tilde{v}_t(l(t),t). \tag{108}$$

We employ a Lyapunov function

$$V_{\tilde{v}}(t) = \frac{1}{2}\left\|\tilde{v}_t(\cdot,t)\right\|^2 + \frac{q}{2}\left\|\tilde{v}_x(\cdot,t)\right\|^2 + \delta_{\tilde{v}}\int_0^{l(t)}(1+x)\tilde{v}_x(x,t)\tilde{v}_t(x,t)dx, \tag{109}$$

where the parameter $\delta_{\tilde{v}}$ is to be determined and needs to at least satisfy $0 < \delta_{\tilde{v}} < 1/(1+L)\min\{1,q\}$ to guarantee the positive definiteness of $V_{\tilde{v}}(t)$. Defining $\Omega_{\tilde{v}}(t)$ as the square of the norm (17), then we can get the inequality

$$\theta_{\tilde{v}1}\Omega_{\tilde{v}}(t) \le V_{\tilde{v}}(t) \le \theta_{\tilde{v}2}\Omega_{\tilde{v}}(t), \tag{110}$$

where

$$\theta_{\tilde{v}1} = \frac{1}{2}[\min\{1,q\} - \delta_{\tilde{v}}(1+L)] > 0,$$
$$\theta_{\tilde{v}2} = \frac{1}{2}[\max\{1,q\} + \delta_{\tilde{v}}(1+L)] > 0.$$

Taking the derivative of $V_{\tilde{v}}(t)$ along the trajectory of the system (107)–(108), we obtain

$$\begin{aligned}\dot{V}_{\tilde{v}} \le& -\frac{\delta_{\tilde{v}}}{2}\left\|\tilde{v}_t\right\|^2 - \frac{\delta_{\tilde{v}}}{2}q\left\|\tilde{v}_x\right\|^2 - \frac{\delta_{\tilde{v}}}{2}\tilde{v}_x^2(0,t)\\ &- \left(a_1q - \frac{\delta_{\tilde{v}}(1+L)}{2}(1+qa_1{}^2)\right)\tilde{v}_t^2(l(t),t)\\ &- \left|\dot{l}(t)\right|\left(\frac{1}{2} + \frac{a_1{}^2q}{2} - a_1\delta_{\tilde{v}}(1+L)\right)\tilde{v}_t^2(l(t),t),\end{aligned} \tag{111}$$

where $0 < l(t) \le L$ is used.

Choosing $\delta_{\tilde{v}}$ to satisfy

$$0 < \delta_{\tilde{v}} < \frac{1}{1+L}\min\left\{1, q, \frac{2a_1q}{1+qa_1^2}, \frac{1+qa_1^2}{2a_1}\right\},$$

then we have

$$\dot{V}_{\tilde{v}} \le -\lambda_{\tilde{v}}V_{\tilde{v}},$$

where $\lambda_{\tilde{v}} = \delta_{\tilde{v}}/(2\theta_{\tilde{v}2}) > 0$. Considering (110), we have $\Omega_{\tilde{v}}(t) \le V_{\tilde{v}}(0)/\theta_{\tilde{v}1}e^{-\lambda_{\tilde{v}}t}$.

The proof is thus completed.

Proof of Lemma 3. According to the system (107)–(108), the e-system can be written as

$$e_{tt}(x,t) = qe_{xx}(x,t), \tag{112}$$
$$e(0,t) = 0, \quad e_x(l(t),t) = -b_1e_t(l(t),t), \tag{113}$$

where

$$b_1 = \frac{qa_1 - |\dot{l}(t)|}{q - qa_1|\dot{l}(t)|}. \tag{114}$$

We can choose $\bar{v}/q < a_1 < 1/\bar{v}$ to ensure $b_1 > 0$, considering $\bar{v}/q < 1/\bar{v}$ in Assumption 2.

Consider a Lyapunov function for the system (112)–(113),

$$V_e(t) = \frac{1}{2}\left\|e_t(\cdot,t)\right\|^2 + \frac{q}{2}\left\|e_x(\cdot,t)\right\|^2 + \delta_e\int_0^{l(t)}(1+x)e_x(x,t)e_t(x,t)dx, \tag{115}$$

where the parameter δ_e is to be determined and needs to at least satisfy $0 < \delta_e < 1/(1+L)\min\{1,q\}$ to guarantee the positive definiteness of $V_e(t)$. Defining $\Omega_e(t)$ as the square of the norm (18), we have the inequality

$$\theta_{e1}\Omega_e(t) \le V_e(t) \le \theta_{e2}\Omega_e(t), \tag{116}$$

where

$$\theta_{e1} = \frac{1}{2}[\min\{1,q\} - \delta_e(1+L)] > 0,$$
$$\theta_{e2} = \frac{1}{2}[\max\{1,q\} + \delta_e(1+L)] > 0.$$

Taking the derivative of $V_e(t)$ along the trajectory of the system (112)–(113), through a similar computation as (111), using (116), we get the exponential stability of the system $e(x,t)$,

$$\dot{V}_e \le -\sigma_{\tilde{d}}V_e, \tag{117}$$

where $\sigma_{\tilde{d}} = \delta_e/(2\theta_{e2})$, and δ_e satisfy:

$$0 < \delta_e < \frac{1}{1+L}\min\left\{1, q, \frac{2b_1 q}{1+qb_1{}^2}, \frac{1+qb_1{}^2}{2b_1}\right\}. \tag{118}$$

We can get

$$\sigma_{\tilde{d}} = \frac{\delta_e}{\max\{1,q\}+\delta_e(1+L)}. \tag{119}$$

From (118) and (119), it can be seen that the decay rate $\sigma_{\tilde{d}}$ is decided by b_1. Combining with (114), we observe that $\sigma_{\tilde{d}}$ depends on a_1.

From (116) and (117), we have

$$\Omega_e(t) \le \frac{V_e(0)}{\theta_{e1}} e^{-\sigma_{\tilde{d}} t}. \tag{120}$$

According to $\tilde{v}$-system (107)–(108), using (120), from the Cauchy–Schwarz inequality, we obtain

$$\begin{aligned}
|\tilde{v}_x(0,t)| &\le |\tilde{v}_x(l(t),t)| + \left|\int_0^{l(t)} \tilde{v}_{xx}(x,t)dx\right| \\
&\le |a_1\tilde{v}_t(l(t),t)| + \frac{\sqrt{L}}{q}\left(\int_0^{l(t)} |\tilde{v}_{tt}(x,t)|^2 dx\right)^{\frac{1}{2}} \\
&= |a_1 e(l(t),t)| + \frac{\sqrt{L}}{q}\|e_t(\cdot,t)\| \le \mu_{\tilde{v}} e^{-\sigma_{\tilde{d}} t},
\end{aligned} \tag{121}$$

where the positive constant $\mu_{\tilde{v}}$ depends only on the initial data. The proof is thus completed.

Proof of Lemma 4. Defining $\bar{y} = e_t$ and taking the derivative of (112)–(113), recalling Assumption 4, we have

$$\bar{y}_{tt}(x,t) = q\bar{y}_{xx}(x,t), \tag{122}$$

$$\bar{y}(0,t) = 0, \quad \bar{y}_x(l(t),t) = -b_2\bar{y}_t(l(t),t), \tag{123}$$

where

$$b_2 = \frac{qb_1 - |\dot{l}(t)|}{q - qb_1|\dot{l}(t)|}. \tag{124}$$

Substituting (114) into (124), we have

$$b_2 = \frac{q(q+|\dot{l}(t)|)a_1 - 2q|\dot{l}(t)|}{q^2 + q|\dot{l}(t)|^2 - 2q^2 a_1|\dot{l}(t)|}.$$

Note that there exists a positive constant a_1 to make $b_2 > 0$. Because there is a mapping relationship between the dependent variable interval $b_1 \in (0,\infty)$ and the independent variable interval $a_1 \in (\bar{v}/q, 1/\bar{v})$ according to the function (114). Therefore, we can choose some a_1 in the range $(\bar{v}/q, 1/\bar{v})$ to make b_1 stay in the range $0 < \bar{v}/q < b_1 < 1/\bar{v} < \infty$ which yields $b_2 > 0$ according to (124).

A calculation similar to (115)–(121), leads to

$$\left|\dot{\tilde{d}}(t)\right| = r|\tilde{v}_{xt}(0,t)| \le \mu_{\tilde{d}_t} e^{-\sigma_{\tilde{d}_t} t},$$

for some positive constants $\sigma_{\tilde{d}_t}$ and $\mu_{\tilde{d}_t}$ which depends on the system initial values only.

Similarly, we can prove the exponential convergence to zero of $\left|\ddot{\tilde{d}}(t)\right| = r|\tilde{v}_{xtt}(0,t)|$.

The proof can then be completed.

Proof of Lemma 6. First, we illustrate well-posedness of the observer error system (40)–(42).

Define an operator $\mathcal{A}$: $D(\mathcal{A}) \to \mathcal{H}$ by

$$\begin{aligned}
&\mathcal{A}(z,v)^T = (v, qz'')^T, \forall (z,v) \in D(\mathcal{A}), \\
&D(\mathcal{A}) = \{(z,v) \in \mathcal{H} | z(0) = v(0) = 0, \\
&\qquad\qquad z'(l(t)) = -a_2 v(l(t))\}.
\end{aligned}$$

The system (41)–(42) can be written as

$$\frac{d}{dt}\begin{pmatrix}\tilde{u}(\cdot,t)\\ \tilde{u}_t(\cdot,t)\end{pmatrix} = \mathcal{A}\begin{pmatrix}\tilde{u}(\cdot,t)\\ \tilde{u}_t(\cdot,t)\end{pmatrix}.$$

Under the boundedness and regularity assumptions (Assumptions 1–2) on $l(t)$, according to Krstic et al. (2008), we can have that $\mathcal{A}$ generates an exponential stable C_0-semigroup, which also can be obtained through the following Lyapunov analysis. Then there exist $\mathcal{K}, \mu_2 > 0$ such that $\|e^{\mathcal{A}t}\| \le \mathcal{K}e^{-\mu_2 t}$. By Weiss and Zhao (2009), it concludes that for any initial values $(\tilde{u}(x,0), \tilde{u}_t(x,0))^T \in \mathcal{H}$, and there exists a unique solution $(\tilde{u}, \tilde{u}_t)^T \in (0,\infty;\mathcal{H})$ to the system (41)–(42) as

$$\begin{pmatrix}\tilde{u}(\cdot,t)\\ \tilde{u}_t(\cdot,t)\end{pmatrix} = e^{\mathcal{A}t}\begin{pmatrix}\tilde{u}(\cdot,0)\\ \tilde{u}_t(\cdot,0)\end{pmatrix}.$$

Considering the ODE (40) which is cascaded with the well-posed PDE-$\tilde{u}$ proved above, it is straightforward to obtain well-posedness of ODE (40). Note that the signal $\tilde{d}(t) = d(t) - \hat{d}(t) = d(t) - (-r\bar{d}_x(0,t))$ in ODE (40) is well-posed, because $\bar{d}_x(0,t)$ is defined by three well-posed systems, where well-posedness of the system-$\bar{d}$ (13)–(15) and the system-$\bar{u}$ (5)–(7) are proved in Krstic et al. (2008), that of the system-u (1)–(3) is proved in Section 5 of Weiss and Zhao (2009). The well-posedness proof of (40)–(42) can then be completed.

Next, we prove the exponential stability of the observer error system (40)–(42) via Lyapunov analysis.

We employ a Lyapunov function

$$V_{\tilde{u}}(t) = \tilde{X}^T(t)P_1\tilde{X}(t) + \phi_{\tilde{u}}E_{\tilde{u}}(t) + \eta_1\tilde{d}(t), \tag{125}$$

where the positive parameters $\phi_{\tilde{u}}$ and η_1 are to be chosen later. The matrix $P_1 = P_1^T > 0$ is the unique solution to the Lyapunov equation

$$P_1(A - \bar{L}C) + (A - \bar{L}C)^T P_1 = -Q_1$$

for some $Q_1 = Q_1{}^T > 0$, and $E_{\tilde{u}}(t)$ is defined as

$$\begin{aligned}
E_{\tilde{u}}(t) = &\frac{1}{2}\left\|\tilde{u}_t(\cdot,t)\right\|^2 + \frac{q}{2}\left\|\tilde{u}_x(\cdot,t)\right\|^2 \\
&+ \delta_{\tilde{u}}\int_0^{l(t)} (1+x)\tilde{u}_x(x,t)\tilde{u}_t(x,t)dx,
\end{aligned} \tag{126}$$

where $\delta_{\tilde{u}}$ should at least satisfy $0 < \delta_{\tilde{u}} < 1/(1+L)\min\{1,q\}$ to guarantee the positive definiteness of $E_{\tilde{u}}(t)$. Defining $\Xi_{\tilde{u}}(t)$ as the square of the system norm (43), similar as (110), we can obtain the following inequality

$$\theta_{\tilde{u}1}\Xi_{\tilde{u}}(t) \le V_{\tilde{u}}(t) \le \theta_{\tilde{u}2}\Xi_{\tilde{u}}(t), \tag{127}$$

with positive constants $\theta_{\tilde{u}1}$ and $\theta_{\tilde{u}2}$.

According to Theorem 1, we obtain

$$\dot{\tilde{d}}(t)^2 = -\sigma_{\tilde{d}}\tilde{d}(t)^2, \tag{128}$$

with the positive $\sigma_{\tilde{d}}$.

Taking the derivative of $V_{\tilde{u}}$ along (40)–(42), (128), applying Young's inequality and $0 < l(t) \le L$, choosing the parameters $\delta_{\tilde{u}}$, η_1 and $\phi_{\tilde{u}}$ to satisfy the following inequalities:

$$0 < \delta_{\tilde{u}} < \frac{1}{1+L}\min\left\{1, q, \frac{2a_2 q}{1+qa_2^2}, \frac{1+qa_2^2}{2a_2}\right\},$$

$$\eta_1 > \frac{8\left|\frac{1}{r}P_1 B\right|^2}{\sigma_{\tilde{d}}\lambda_{\min}(Q_1)}, \quad \phi_{\tilde{u}} > \frac{4|P_1 B|^2}{q\delta_{\tilde{u}}\lambda_{\min}(Q_1)},$$

we arrive at

$$\dot{V}_{\tilde{u}} \le -\sigma_{\tilde{u}} V_{\tilde{u}}, \tag{129}$$

where

$$\sigma_{\tilde{u}} = \frac{1}{\theta_{\tilde{u}2}} \min\left\{ \frac{\delta_{\tilde{u}}}{2}\phi_{\tilde{u}}, \frac{\delta_{\tilde{u}}}{2} q\phi_{\tilde{u}}, \frac{1}{2}\lambda_{\min}(Q_1), \eta_1\sigma_{\tilde{d}} - \frac{4\left|\frac{1}{r}P_1 B\right|^2}{\lambda_{\min}(Q_1)} \right\} > 0. \tag{130}$$

The proof of Lemma 6 is completed.

Proof of Lemma 7. First, we illustrate well-posedness of the target system-$(\hat{w}, \hat{X})$ (58)–(61).

Define an operator $\mathcal{A}_1$: $D(\mathcal{A}_1) \to \mathcal{H}$ by

$$\mathcal{A}_1(z, v)^T = (v, qz'')^T, \forall (z, v) \in D(\mathcal{A}_1),$$
$$D(\mathcal{A}_1) = \{(z, v) \in \mathcal{H} | z(0) = v(0) = 0, z'(l(t)) = -a_3 v(l(t))\}.$$

The system (59)–(61) can be written as

$$\frac{d}{dt}\begin{pmatrix} \hat{w}(\cdot, t) \\ \hat{w}_t(\cdot, t) \end{pmatrix} = \mathcal{A}_1 \begin{pmatrix} \hat{w}(\cdot, t) \\ \hat{w}_t(\cdot, t) \end{pmatrix} + \begin{pmatrix} 0 \\ f(\cdot, t) \end{pmatrix} + \mathcal{B}C\tilde{X}(t),$$

where $f(x, t) = -\bar{f}_1(x)\tilde{X}(t) + \bar{\eta}(x, t)$ and $\mathcal{B} = (0, \delta(x))^T$. Similar to $\mathcal{A}$ in Lemma 6, $\mathcal{A}_1$ generates an exponential stable C_0-semigroup, which also can be obtained through the following Lyapunov analysis. Then there exist $\mathcal{K}_1$, $\mu_3 > 0$ such that $\|e^{\mathcal{A}_1 t}\| \le \mathcal{K}_1 e^{-\mu_3 t}$.

It is a routine exercise that $\mathcal{B}$ is admissible for $\mathcal{A}_1$. By Weiss and Zhao (2009), recalling Lemma 6 and (62), it concludes that for any initial values $(\hat{w}(x, 0), \hat{w}_t(x, 0))^T \in \mathcal{H}$, and there exists a unique solution $(\hat{w}, \hat{w}_t)^T \in C(0, \infty; \mathcal{H})$ to the system (59)–(61) as

$$\begin{pmatrix} \hat{w}(\cdot, t) \\ \hat{w}_t(\cdot, t) \end{pmatrix} = e^{\mathcal{A}_1 t}\begin{pmatrix} \hat{w}(\cdot, 0) \\ \hat{w}_t(\cdot, 0) \end{pmatrix} + \int_0^t e^{\mathcal{A}_1(t-s)}\begin{pmatrix} 0 \\ f(\cdot, s) \end{pmatrix} ds + \int_0^t e^{\mathcal{A}_1(t-s)}\mathcal{B}C\tilde{X}(s)ds.$$

Considering the ODE (58) which is cascaded with the well-posed PDE-$\hat{w}$ proved above. It is straightforward to obtain well-posedness of the ODE (58). Note that the signal $\tilde{Z}(t)$ in the ODE (58) depends the ODE-$\hat{Y}$ (24) which is an obviously well-posed system. The well-posedness proof of (58)–(61) can then be completed.

Next, we prove the target system-$(\hat{w}, \hat{X})$ (58)–(61) is exponentially stable in the sense of (65) via Lyapunov analysis.

Let $V_{\hat{w}}(t)$ be a Lyapunov function as

$$V_{\hat{w}}(t) = \hat{X}^T(t)P_2\hat{X}(t) + \phi_{\hat{w}}E_{\hat{w}}(t) + \xi_3\bar{\eta}_m(t)^2 + \xi_4\tilde{d}(t)^2 + \xi_5\left|\tilde{Z}(t)\right|^2 \tag{131}$$

where the matrix $P_2 = P_2^T > 0$ is the unique solution to the following Lyapunov equation

$$P_2(A + BK) + (A + BK)^T P_2 = -Q_2,$$

for some matrix $Q_2 = Q_2{}^T > 0$. $E_{\hat{w}}(t)$ in (131) is defined as

$$E_{\hat{w}}(t) = \frac{1}{2}\left\|\hat{w}_t(\cdot, t)\right\|^2 + \frac{q}{2}\left\|\hat{w}_x(\cdot, t)\right\|^2 + \delta_{\hat{w}}\int_0^{l(t)}(1 + x)\hat{w}_x(x, t)\hat{w}_t(x, t)dx, \tag{132}$$

where the parameter $\delta_{\hat{w}}$ is to be determined and needs to at least satisfy $0 < \delta_{\hat{w}} < 1/(1 + L)\min\{1, q\}$ to guarantee the positive definiteness of $E_{\hat{w}}(t)$. The positive parameters $\phi_{\hat{w}}$ and ξ_3, ξ_4, ξ_5 are to be chosen later.

Defining $\Xi_{\hat{w}}(t)$ as the square of the system norm (65), similar as (110), there exist two positive constants $\theta_{\hat{w}1}$, $\theta_{\hat{w}2}$ to hold that

$$\theta_{\hat{w}1}\Xi_{\hat{w}}(t) \le V_{\hat{w}}(t) \le \theta_{\hat{w}2}\Xi_{\hat{w}}(t). \tag{133}$$

Taking the derivative of $V_{\hat{w}}$ along (58)–(61) and recalling (28), (128) and (64), applying Young's inequality, through the similar computation of (125)–(130), with (65), (133), we arrive at

$$\dot{V}_{\hat{w}} \le -\sigma_{\hat{w}}V_{\hat{w}} + \xi_2\left|\tilde{X}(t)\right|^2, \tag{134}$$

where

$$\sigma_{\hat{w}} = \frac{1}{\theta_{\hat{w}2}}\min\left\{\frac{1}{4}\phi_{\hat{w}}\delta_{\hat{w}}, \frac{1}{2}q\phi_{\hat{w}}\delta_{\hat{w}}, \xi_3\sigma_{\bar{\eta}} - \frac{C_{max}^2 L}{4r_0}, \frac{1}{2}\lambda_{\min}(Q_2), \xi_4\sigma_{\tilde{d}} - \frac{8|P_2 B|}{r^2\lambda_{\min}(Q_2)}, \xi_5\sigma_{\tilde{Z}} - \frac{8|P_2 B C_z|}{r^2\lambda_{\min}(Q_2)}\right\} > 0,$$

and

$$\xi_2 = \frac{1}{4}\phi_{\hat{w}}{}^2 + \frac{1}{2}\phi_{\hat{w}}{}^2 C^2(A - \bar{L}C)^2 + \frac{4\left|P_2(\bar{L}C + B\gamma(0, 0)C)\right|^2}{\lambda_{\min}(Q_2)}.$$

The parameters ξ_3, ξ_4, ξ_5, $\delta_{\hat{w}}$, $\phi_{\hat{w}}$, r_0 should satisfy:

$$\xi_3 > \frac{C_{max}^2 L}{4r_0\sigma_{\bar{\eta}}}, \xi_4 > \frac{8|P_2 B|}{\sigma_{\tilde{d}} r^2\lambda_{\min}(Q_2)}, \xi_5 > \frac{8|P_2 B C_z|}{\sigma_{\tilde{Z}} r^2\lambda_{\min}(Q_2)},$$
$$0 < \delta_{\hat{w}} < \frac{1}{1 + L}\min\left\{1, q, \frac{2a_3 q}{1 + qa_3^2}, \frac{1 + qa_3^2}{2a_3}\right\},$$
$$\phi_{\hat{w}} > \frac{2}{\delta_{\hat{w}}}\max\left\{2C_1 L, \frac{q}{2} + \frac{4|P_2 B|^2}{q\lambda_{\min}(Q_2)}\right\},$$
$$0 < r_0 < \frac{1}{4}\phi_{\hat{w}}\delta_{\hat{w}} - C_1 L,$$

where $C_1 = \max_{x\in[0,L]}\left\{\left|\bar{f}_1(x)\right|^2\right\}$.

Considering the observer error system (40)–(42), the Lyapunov function $V(t)$ of the overall $(\tilde{X}, \tilde{u}, \hat{X}, \hat{w})$-system is chosen as

$$V(t) = \lambda V_{\tilde{u}}(t) + V_{\hat{w}}(t), \tag{135}$$

where a positive constant λ is to be determined. Taking the derivative of (135) and using (127), (129), (134), we get

$$\dot{V} \le -\frac{\lambda\sigma_{\tilde{u}}}{2}V_{\tilde{u}} - \sigma_{\hat{w}}V_{\hat{w}} - \left(\frac{\lambda\sigma_{\tilde{u}}\theta_{\tilde{u}2}}{2} - \xi_2\right)\left|\tilde{X}(t)\right|^2. \tag{136}$$

Choosing λ sufficiently large, we arrive at

$$\dot{V} \le -\frac{\lambda\sigma_{\tilde{u}}}{2}V_{\tilde{u}} - \sigma_{\hat{w}}V_{\hat{w}} \le -\sigma V, \tag{137}$$

where

$$\sigma = \min\{\frac{\sigma_{\tilde{u}}}{2}, \sigma_{\hat{w}}\} > 0. \tag{138}$$

The proof of Lemma 7 is completed.

Proof of Lemma 9. Differentiating (59) with respect to x, differentiating (60)–(61) with respect to t, we have

$$\hat{w}_{ttx}(x, t) = q\hat{w}_{xxx}(x, t) - \bar{f}_1'(x)\tilde{X}(t) + \bar{\eta}_x(x, t), \tag{139}$$
$$\hat{w}_t(0, t) = C(A - \bar{L}C)\tilde{X}(t), \tag{140}$$
$$\hat{w}_{tt}(l(t), t) = -b_3\hat{w}_{xt}(l(t), t) - \frac{\bar{f}_1(x)}{a_3 q + \dot{l}(t)}\tilde{X}(t) + \frac{1}{a_3 q + \dot{l}(t)}\bar{\eta}(x, t), \tag{141}$$

where $b_3 > 0$ by choosing $\bar{v}/q < a_3 < 1/\bar{v}$. We know $\bar{\eta}(x, t)$ is exponentially convergent to zero. Similarly, we obtain $\bar{\eta}_x(x, t)$ is also exponentially convergent to zero by using (62), (63) and Theorem 1, Lemma 4, Lemma 5. According to Lemma 6, we know $\tilde{X}(t)$ is exponentially convergent to zero. Through a similar calculation with the proof of Lemma 7, we can obtain the exponential stability of the system (139)–(141) in the sense of $\|\hat{w}_{xt}(\cdot, t)\|^2 + \|\hat{w}_{xx}(\cdot, t)\|^2$. Due to the space limitations, we omit the lengthy calculation process.

Through the invertible transformations (57), we could get an exponential stability estimate for the norm $(\|\hat{z}_{xt}(\cdot, t)\|^2$

$+ \|\hat{z}_{xx}(\cdot,t)\|^2)^{1/2}$. Recalling the transformation (49), we have

$$\left\|\hat{u}_{xx}(\cdot,t)\right\|^2 \le 2\left\|\hat{z}_{xx}(\cdot,t)\right\|^2 + 2L\left|\vartheta_m''\hat{Z}(t)\right|^2,$$
$$\left\|\hat{u}_{xt}(\cdot,t)\right\|^2 \le 2\left\|\hat{z}_{xt}(\cdot,t)\right\|^2 + 2L\left|\vartheta_m'\dot{\hat{Z}}(t)\right|^2,$$

where $\vartheta_m'' = \max_{x\in[0,L]}\{|\vartheta''(x)|\}$, $\vartheta_m' = \max_{x\in[0,L]}\{|\vartheta'(x)|\}$.

$|\vartheta_m''\hat{Z}(t)|$ and $|\vartheta_m'\dot{\hat{Z}}(t)| = |\vartheta_m'||\hat{C}[(\hat{A}_z - L_z\hat{C}_z)\hat{Y}(t) - L_z r\bar{d}_x(0,t)]|$ are bounded. We thus obtain the bounded estimates for the norm $(\|\hat{u}_{xt}(\cdot,t)\|^2 + \|\hat{u}_{xx}(\cdot,t)\|^2)^{1/2}$.

The proof of Lemma 9 is completed.

References

Bekiaris-Liberis, N., & Krstic, M. (2018). Compensation of transport actuator dynamics with input-dependent moving controlled boundary. *IEEE Transactions on Automatic Control*.

Cai, X., & Krstic, M. (2016). Nonlinear stabilization through wave PDE dynamics with a moving uncontrolled boundary. *Automatica*, *68*, 27–38.

Diagne, M., Bekiaris-Liberis, N., & Krstic, M. (2017). Time-and state-dependent input selay-compensated bang–bang control of a screw extruder for 3d printing. *International Journal of Robust and Nonlinear Control*, *27*, 3727–3757.

Feng, H., & Guo, B. Z. (2017). A new active disturbance rejection control to output feedback stabilization for a one-dimensional anti-stable wave equation with disturbance. *IEEE Transactions on Automatic Control*, *62*, 3774–3787.

Francis, B. A., & Wonham, W. M. (1976). The internal model principle of control theory. *Automatica*, *12*, 457–465.

Gugat, M. (2007a). Optimal boundary feedback stabilization of a string with moving boundary. *IMA Journal of Mathematical Control and Information*, *25*, 111–121.

Gugat, M. (2007b). Optimal energy control in finite time by varying the length of the string. *SIAM Journal on Control and Optimization*, *46*, 1705–1725.

Guo, B. Z., & Jin, F. F. (2013a). The active disturbance rejection and sliding mode control approach to the stabilization of the Euler–Bernoulli beam equation with boundary input disturbance. *Automatica*, *49*, 2911–2918.

Guo, B. Z., & Jin, F. F. (2013b). Sliding mode and active disturbance rejection control to stabilization of one-dimensional anti-stable wave equations subject to disturbance in boundary input. *IEEE Transactions on Automatic Control*, *58*, 1269–1274.

Guo, B. Z., & Jin, F. F. (2015). Output feedback stabilization for one-dimensional wave equation subject to boundary disturbance. *IEEE Transactions on Automatic Control*, *60*, 824–830.

Guo, B. Z., & Liu, J. J. (2014). Sliding mode control and active disturbance rejection control to the stabilization of one-dimensional schrödinger equation subject to boundary control matched disturbance. *International Journal of Robust and Nonlinear Control*, *24*, 2194–2212.

Guo, B. Z., & Wu, Z. H. (2017). Output tracking for a class of nonlinear systems with mismatched uncertainties by active disturbance rejection control. *Systems & Control Letters*, *100*, 21–31.

Guo, B. Z., & Zhou, H. C. (2015). The active disturbance rejection control to stabilization for multi-dimensional wave equation with boundary control matched disturbance. *IEEE Transactions on Automatic Control*, *60*, 143–157.

Guo, W., & Guo, B. Z. (2013a). Adaptive output feedback stabilization for one-dimensional wave equation with corrupted observation by harmonic disturbance. *SIAM Journal on Control and Optimization*, *51*, 1679–1706.

Guo, W., & Guo, B. Z. (2013b). Parameter estimation and non-collocated adaptive stabilization for a wave equation subject to general boundary harmonic disturbance. *IEEE Transactions on Automatic Control*, *58*, 1631–1643.

Guo, W., & Guo, B. Z. (2013c). Stabilization and regulator design for a one-dimensional unstable wave equation with input harmonic disturbance. *International Journal of Robust and Nonlinear Control*, *23*, 514–533.

Guo, W., & Guo, B. Z. (2016). Performance output tracking for a wave equation subject to unmatched general boundary harmonic disturbance. *Automatica*, *68*, 194–202.

Guo, W., Shao, Z. C., & Krstic, M. (2017). Adaptive rejection of harmonic disturbance anticollocated with control in 1D wave equation. *Automatica*, *79*, 17–26.

Han, J. (2009). From PID to active disturbance rejection control. *IEEE Transactions on Industrial Electronics*, *56*, 900–906.

He, W., & Ge, S. S. (2016). Cooperative control of a nonuniform gantry crane with constrained tension. *Automatica*, *66*, 146–154.

Isidori, A., Marconi, L., & Serrani, A. (2012). *Robust autonomous guidance: An internal model approach*. Springer.

Kaczmarczyk, S., & Ostachowicz, W. (2003). Transient vibration phenomena in deep mine hoisting cables. Part 1: Mathematical model. *Journal of Sound and Vibration*, *262*, 219–244.

Kang, W., & Fridman, E. (2016). Sliding mode control of Schrodinger equation-ODE in the presence of unmatched disturbances. *Systems & Control Letters*, *98*, 65–73.

Koga, S., Diagne, M., & Krstic, M. (2016). Output feedback control of the one-phase Stefan problem. In *IEEE conference on decision and control* (pp. 526–531).

Krstic, M. (2009). Compensating a string PDE in the actuation or sensing path of an unstable ODE. *IEEE Transactions on Automatic Control*, *54*, 1362–1368.

Krstic, M., Guo, B.-Z., Balogh, A., & Smyshlyaev, A. (2008). Output-feedback stabilization of an unstable wave equation. *Automatica*, *44*, 63–74.

Krstic, M., & Smyshlyaev, A. (2008). *Boundary control of PDEs: A course on backstepping designs*. Singapore: SIAM.

Li, S., Yang, J., Chen, W. H., & Chen, X. (2012). Generalized extended state observer based control for systems with mismatched uncertainties. *IEEE Transactions on Industrial Electronics*, *59*, 4792–4802.

Mciver, D. B. (1973). Hamilton's principle for systems of changing mass. *Journal of Engineering Mathematics*, *7*(3), 249–261.

Rebarber, R., & Weiss, G. (2003). Internal model based trackingand disturbance rejection for stable well-posed systems. *Automatica*, *39*, 1555–1569.

Tang, S.-X., Guo, B. Z., & Krstic, M. (2014). Active disturbance rejection control for a 2×2 hyperbolic system with an input disturbance. *IFAC Proceedings Volumes*, *47*, 11385–11390.

Tang, S.-X., & Xie, C. (2011). State and output feedback boundary control for a coupled PDE–ODE system. *Systems Control Letters*, *60*, 540–545.

Wang, J. M., Liu, J. J., Ren, B., & Chen, J. H. (2015). Sliding mode control to stabilization of cascaded heat PDE–ODE systems subject to boundary control matched disturbance. *Automatica*, *52*, 23–34.

Wang, J., Pi, Y., Hu, Y., & Gong, X. (2017). Modeling and dynamic behavior analysis of a coupled multi-cable double drum winding hoister with flexible guides. *Mechanism and Machine Theory*, *108*, 191–208.

Wang, J., Tang, S.-X., Pi, Y., & Krstic, M. (2017). Disturbance estimation of a wave pde on a time-varying domain. In *2017 Proceedings of the conference on control and its applications* (pp. 107–111). SIAM.

Wang, J., Koga, S., Pi, Y., & Krstic, M. (2018). Axial vibration suppression in a partial differential equation model of ascending mining cable elevator. *ASME Journal of Dynamic Systems, Measurement and Control*, *140*(11), 111003.

Weiss, G., & Zhao, X. (2009). Well-posedness and controllability of a class of coupled linear systems. *SIAM Journal on Control and Optimization*, *48*(4), 2719–2750.

Xue, W., & Huang, Y. (2014). On performance analysis of ADRC for a class of MIMO lower-triangular nonlinear uncertain systems. *ISA Transactions*, *53*, 955–962.

Zhou, H. C., Guo, B. Z., & Wu, Z. H. (2016). Output feedback stabilisation for a cascaded wave PDE-ODE system subject to boundary control matched disturbance. *International Journal of Control*, *89*, 2396–2405.

Zhou, Z., & Tang, S.-X. (2012). Boundary stabilization of a coupled wave-ODE system with internal anti-damping. *International Journal of Control*, *85*, 1683–1693.

Zhu, W., & Ni, J. (2000). Energetics and stability of translating media with an arbitrarily varying length. *Journal of Vibration and Acoustics*, *122*, 295–304.

Ji Wang received the B.Eng. degree in Mechanical Engineering and Automation from Jimei University, Xiamen, China, in 2012. From 2012 to 2014, he was a master student in Mechatronic Engineering at Chongqing University, Chongqing, China, where he has been a Ph.D. student in Mechanical Engineering from 2014. Supported by China Scholarship Council, he was a visiting graduate student in the Department of Mechanical and Aerospace Engineering at University of California, San Diego, La Jolla, CA, USA, from 2015 to 2017. His research interests include modeling and control of distributed parameter systems, active disturbance rejection control and adaptive control, with applications in mechanical systems.

Shu-Xia Tang received her Ph.D. in Mechanical Engineering in 2016 from the Department of Mechanical & Aerospace Engineering, University of California, San Diego, USA. She is currently a postdoctoral research fellow at the Institute of Transportation Studies and the Department of Civil and Environmental Engineering, University of California, Berkeley, USA and Inria Sophia Antipolis — Méditerranée, France. Her main research interests are modeling, stability analysis, estimation and control design of distributed parameter systems.

Yangjun Pi received the B.Eng. degree in Mechatronic Engineering and the Ph.D. degree in Mechanical Engineering from Zhejiang University, Hangzhou, China, in 2005 and 2010 respectively. Currently, he is an associate professor in the State Key Laboratory of Mechanical Transmission, Chongqing University, Chongqing, China. His research interests include control of distributed parameter systems, vibration control.

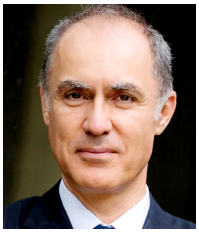

Miroslav Krstic is Distinguished Professor of Mechanical and Aerospace Engineering, holds the Alspach endowed chair, and is the founding director of the Cymer Center for Control Systems and Dynamics at UC San Diego. He also serves as Associate Vice Chancellor for Research at UCSD. As a graduate student, Krstic won the UC Santa Barbara best dissertation award and student best paper awards at CDC and ACC. Krstic has been elected Fellow of seven scientific societies – IEEE, IFAC, ASME, SIAM, AAAS, IET (UK), and AIAA (Assoc. Fellow) – and as a foreign member of the Academy of Engineering of Serbia. He has received the ASME Oldenburger Medal, Nyquist Lecture Prize, Paynter Outstanding Investigator Award, Ragazzini Education Award, Chestnut textbook prize, the PECASE, NSF Career, and ONR Young Investigator awards, the Axelby and Schuck paper prizes, and the first UCSD Research Award given to an engineer. Krstic has also been awarded the Springer Visiting Professorship at UC Berkeley, the Distinguished Visiting Fellowship of the Royal Academy of Engineering, the Invitation Fellowship of the Japan Society for the Promotion of Science, and honorary professorships from four universities in China. He serves as Senior Editor in IEEE Transactions on Automatic Control and Automatica, as editor of two Springer book series, and has served as Vice President for Technical Activities of the IEEE Control Systems Society and as chair of the IEEE CSS Fellow Committee. Krstic has coauthored twelve books on adaptive, nonlinear, and stochastic control, extremum seeking, control of PDE systems including turbulent flows, and control of delay systems.